NSTX Upgrade

Analysis of Diagnostic and Diagnostic Shutter

NSTXU-CALC-40-01-00

Rev 0

July 2011

Prepared By:

Peter Titus

Digitally signed by Peter Titus
DN: cn=Peter Titus, o, ou, email=ptitus@pppl.gov, c=US
Date: 2011.11.11 08:47:52 -05'00'

Peter Titus for Joseph Boales (Drexel Co-op Student)

Reviewed By:

Yuhu Zhai

Digitally signed by Yuhu Zhai
DN: cn=Yuhu Zhai, o=PPPL, ou=Mechanical Engineering, email=yzhai@pppl.gov, c=US
Date: 2011.11.11 09:23:56 -05'00'

Yuhu Zhai, Engineering Analysis Division

Reviewed By:

Robert Kaita

Digitally signed by Robert Kaita
cn=Robert Kaita, o= Princeton Plasma Physics Laboratory, l= Princeton, st= New Jersey, c= US, email= kaita@pppl.gov
Date: 2011.11.10 16:25:18 EST

Robert Kaita, Cognizant Engineer

PPPL Calculation Form

Calculation # **NSTXU-CALC-40-01** Revision # **00** WP : **1511**

Purpose of Calculation:

The purpose of this calculation is to survey the existing NSTX diagnostics and look for components that would be sensitive to the increased thermal and electromagnetic loading planned for the upgrade, Also the purpose of this analysis is to qualify the diagnostics and the diagnostic shutters for the larger disruption loads, heat loads, and any other factors that may present a problem to the function of the diagnostic systems.

References (List any source of design information including computer program titles and revision levels.)

See the body of the calculation

Assumptions (Identify all assumptions made as part of this calculation.)

The primary assumption is that the existing diagnostics represent the diagnostics that will be installed in the upgrade. The information and conclusions in theis calculations must be reviewed for applicability as the diagnostics are re-installed in the upgrade machine.

Calculation (Calculation is either documented here or attached)

See the body of the calculation, and database

Conclusion (Specify whether or not the purpose of the calculation was accomplished.)

The diagnostics have been tabulated and described in a database created using Microsoft Access. This database describes the diagnostic, the ways in which it is most likely to be affected by the NSTX-CSU, and other attributes of the diagnostic. It is a living document in that it can be updated as more information becomes available or more information is discovered about the operation of each diagnostic. Using this database, each diagnostic has its own data sheet. These data sheets can be easily manipulated and edited by those with a basic knowledge of Microsoft Access. The entire database can also be exported as a Microsoft Excel table if desired. The data sheets can also be exported as PDF documents. In the Recommendations section of the calculation some recommendations have been provided in Table 2. General recommendations have also been made throughout the datasheets and for problems that may arise though they were not anticipated for a particular diagnostic.

Cognizant Engineer's printed name, signature, and date

Robert Kaita

Digitally signed by Robert Kaita
cn=Robert Kaita, o= Princeton Plasma Physics Laboratory, l= Princeton, st= New Jersey, c= US, email= kaita@pppl.gov
Date: 2011.11.10 16:26:32 EST

I have reviewed this calculation and, to my professional satisfaction, it is properly performed and correct.

Checker's printed name, signature, and date

Yuhu Zhai

Digitally signed by Yuhu Zhai
DN: cn=Yuhu Zhai, o=PPPL, ou=Mechanical Engineering, email=yzhai@pppl.gov, c=US
Date: 2011.11.11 09:24:09 -05'00'

Executive Summary

The purpose of this analysis is to qualify the diagnostics and the diagnostic shutters for the larger disruption loads, heat loads, and any other factors that may present a problem to the function of the diagnostic systems. The diagnostics have been tabulated and described in a database created using Microsoft Access. This database describes the diagnostic, the ways in which it is most likely to be affected by the NSTX-CSU, and other attributes of the diagnostic. It is a living document in that it can be updated as more information becomes available or more information is discovered about the operation of each diagnostic. Using this database, each diagnostic has its own data sheet. These data sheets can be easily manipulated and edited by those with a basic knowledge of Microsoft Access. The entire database can also be exported as a Microsoft Excel table if desired. The data sheets can also be exported as PDF documents.

Eddy current analyses have also been performed for each of the shutter types and most have been done several times using different magnetic field configurations. The background magnetic field and the change in magnetic field at each location was read from a table and written into an ANSYS script. The script imports a shutter from an .iges file and imposes an initial and a final vector potential to calculate the eddy currents. The model is meshed within the script using SOLID 97. The material properties used are generally those of 304 Stainless Steel, though they vary in some cases. The eddy current densities matched with approximate values which were calculated by hand. The results from the eddy current calculation are then read into a structural model (which is meshed using SOLID 45), where the stresses and deflections in the shutters are calculated.

In order to qualify the shutters for the higher heat flux, I wrote a script in Python (based on one written in True Basic). The script calculates the ratcheted temperature of the shutter. The heat flux and material properties of the shutter can be easily manipulated in this script. Also, the shutters were run through an ANSYS script, similar to the one mentioned above, except that the model is first meshed with SOLID 70 and a heat flux, rather than a vector potential, is imposed on the front surface of the model. The ANSYS model only shows the effect that a single pulse of the machine has on the shutter. Multiple pulses would not be necessary for the shutters because the temperature of the shutter quickly equilibrates because it is so thin.

Table of Contents

Table of Figures

Summary of Diagnostics

For the NSTX diagnostics, a database was created to document each of the diagnostics and the effects that the NSTX-CSU may have on them. Some of the topics included in the database include whether the diagnostic is sensitive to disruption loads, heat loads, or radiation levels. A sample entry in this database can be seen on the right. The database is a living document that can be updated as more information is discovered or becomes available. Table 1, below, lists the diagnostics and the most likely cause(s) for concern for each diagnostic if there are any. The most likely causes are taken directly from the database. A sample entry in this database can be seen on the right. The database is a living document that can updated as more information is discovered or becomes available.

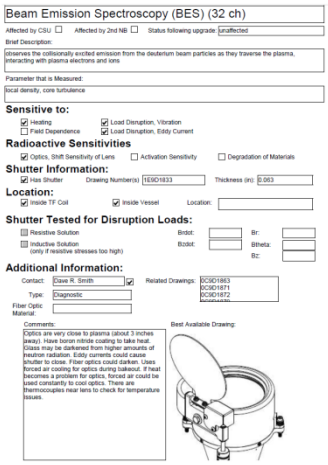

Figure 1. Sample entry in diagnostics database.

Table 1. ***List of diagnostics and the most likely cause for concern and relevant comments for each diagnostic.***

Diagnostic	Causes for Concern/Comments
"Optical" soft x-ray array	None. Diagnostic is being replaced.
1-D CCD Hα cameras (divertor, midplane)	See General Concerns for Cameras
2-D divertor fast visible camera	See General Concerns for Cameras
Beam Emission Spectroscopy (BES) (32 ch)	Uses forced air cooling for optics during bakeout. If heating becomes a problem, cooling could be used constantly. Glass for optics could be darkened by radiation.
Biased Electrode and Probe (BEAP)	Should be unaffected. Will also be modified before upgrade.
Charge-Exchange Recombination Spectroscopy (CHERS): Ti(R) and VΦ(r) (51 ch)	Optics could be darkened by radiation.
Diamagnetic flux measurement	None. If loop is installed, it will be designed with upgrade in mind.
Divertor bolometer (20 ch)	See General Concerns for Cameras
Edge deposition monitors	Window could be darkened by radiation.
Edge Neutral Density Diagnostic (ENDD)	See General Concerns for Cameras
Edge neutral pressure gauges	None.
Edge Rotation Diagnostics (Ti, VΦ, Vppol)	Optics could darken from radiation.
Fast camera view of RF antennas	See General Concerns for Cameras
Fast ion D-α diagnostic	Should check supports for vibrations during disruption.
Fast IR Camera	Already becomes activated. Higher radiation dose will be

	worse. Also, increase in noise.
Fast lost-ion probe	Radiation could darken glass.
Fast visible camera	See General Concerns for Cameras
Fission chamber neutron measurement	None.
Gas-puff Imaging (2msec)-midplane and divertor	Shielding for electronics may need to be increased. Fiber optics may darken.
Halo Tile current detectors	Thermally isolated. Could be a problem.
High-n and high-frequency Mirnov arrays	Saturation of digitizers.
Interferometry/forward scattering (1 mm, 1ch)	G10 base could become activated.
IR cameras (30 Hz) (3)	None. Also used on high radiation machines such as DIII-D.
Langmuir probe array-inter-LLD	Designed for 10 MW/m2 for 1 second. May need to be replaced anyway.
Langmuir probes-outboard edge	May need to be replaced when CS is taken out.
Langmuir probes-PFC tiles	On CS. Being replaced.
Langmuir probes-RF antenna	May need to be replaced when CS is taken out.
LLNL EUV spectrometer LoWEUS	None.
LLNL EUV spectrometer XEUS	Being relocated. No other concerns.
Locked-mode detectors	Possible saturation of digitizers. Detectors need to be relocated. Extra PF supports may interact with sensors.
Magnetics for equilibrium reconstruction	High heat fluxes may make diagnostics more difficult. Would be a nuisance, but not a problem. Mounting techniques may need to be modified because of high heat fluxes.
Microwave reflectometers (65 GHz backscattering, correlation, FM/CW, fixed frequency)	Window could darken. Copper pipes could bend from larger eddy currents (has happened before). Teflon connector cables could degrade.
Midplane tangential bolometer array	See General Concerns
Motional Stark Effect based on Collisionally-Induced Fluorescence	May need to clean window more often because of longer run time. Noise problems could worsen. Fibers could darken.
Motional Stark Effect based on Laser-Induced Fluorescence	Noise problems may worsen. Sightlines blocked by extension of beam armor.
Multi-pulse Thomson scattering (30 ch, 60 Hz)	May not be able to take measurement at 10 keV at higher temperatures. More noise and saturation problems. G10 components become activated. Vinyl and PVC could degrade.
Neutron detectors (2 uranium and 4 fast scintillator)	Will need to add another channel to accommodate higher neutron flux.
P-CHERS: Vθ(r) (75 ch)	Optics could be darkened.
Plasma TV	See General Concerns for Cameras
RF Antenna (ECH Launcher)	Most of the heat is taken by the boron nitride section.
RF edge magnetic probe	Shielded by tiles. Can be adjusted if they are too close to plasma.

RWM Coils	Should be checked for effects of eddy currents and vibrations.
RWM sensors (n = 1, 2, and 3)	Could be bent by forces induced by halo currents. May saturate digitizers.
Sample probe	Samples may become activated. Can be a nuisance, but not a problem.
Scrape-off layer reflectometer	Similar problems to microwave reflectometer.
SWIFT 2-D flow diagnostic	See General Concerns for Cameras
Tile temperature thermocouple array	Array on center stack will be replaced. Should be designed with upgrade in mind.
Ultra-soft x-ray arrays - tomography	Eddy currents could present a problem. May need stronger supports that can take a larger load. Noise from SPA's is an issue. Adding more will make it worse.
UV survey spectrometer (SPRED)	To be relocated.
Vertical x-ray crystal spectrometer	None.
Visible (VIPS) survey spectrometer	Fiber optics could darken.
Visible bremsstrahlung detector (1 ch)	Window could be darkened. New beam dump needed (geometrical reasons).
Visible filterscopes	Fiber optics could darken.
VUV transmission grating spectrometer	Currently well-supported, though more supports may be desired. Fast cameras may be added.
Wall coupon analysis	Wall supports should be checked. Activation would be a nuisance.

General Concerns for Diagnostics

Several of the diagnosticians expressed concerns that could affect many of the diagnostics. They are listed below:

- The spa's (fast switching power supplies) create noise for the diagnostics. If more are needed, there will be more noise.
- Wire fatigue could be a problem for vessel-mounted diagnostics from more vibration.
- Saturation of digitizers could occur because of larger magnetic fields.
- More deposition (lithium, carbon, etc.) on glass from longer shots could cause problems for diagnostics.

There was also a concern that does not directly affect diagnostics, but may be important to correct since the radiation levels are expected to rise by a factor of 50. The test cell wall penetrations are drilled straight through (line of sight) the wall, allowing radiation to directly penetrate the wall. The holes should be drilled at angles to prevent radiation from penetrating.

General Concerns for Cameras

There are also concerns that will mostly affect cameras. First, any glass fiber optics or windows may darken much more quickly. If the darkening occurs too quickly, they should be replaced with quartz. Also, any cameras that use a silicon chip may need better shielding to prevent additional noise.

Diagnostic Shutters

The diagnostic shutters were analyzed (see *ANSYS Analysis of Shutters*) for the stresses that develop from eddy currents as well as their deflections due to these stresses. Thermal analyses were done to check for deflection. The eddy current analyses were done in ANSYS using the resistive solution, since this is the worst-case solution. One such analysis can be seen on the left. If the stresses that develop due to the resistive solution are too large, the inductive solution will also be checked for a more realistic comparison. The thermal analysis will be done using ANSYS and using a simple script written in Python to model the ratcheting of the temperature.

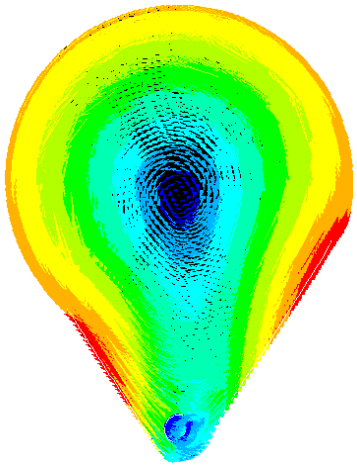

Figure 2. Sample eddy current distribution due to the worst case disruption.

Recommendations

For each of the diagnostics, I have made some recommendations if necessary. These recommendations are in Table 2. I have also made general recommendations for problems that may arise though they were not anticipated for a particular diagnostic.

Table 2. List of diagnostics and recommendations for each diagnostic, if any.

Diagnostic	Recommendations
"Optical" soft x-ray array	None.
1-D CCD Hα cameras (divertor, midplane)	See *General Recommendations.*
2-D divertor fast visible camera	May need more mechanical support. See *General Recommendations.*
Beam Emission Spectroscopy (BES) (32 ch)	Replace all glass with quartz if glass darkens. Constantly use cooling if heat becomes a problem.
Biased Electrode and Probe (BEAP)	None.
Charge-Exchange Recombination Spectroscopy (CHERS): Ti(R) and VΦ(r) (51 ch)	Replace glass fiber optics with quartz if darkening becomes a problem.
Diamagnetic flux measurement	None.
Divertor bolometer (20 ch)	See *General Recommendations.*
Edge deposition monitors	Replace window with quartz if darkening occurs.
Edge Neutral Density Diagnostic (ENDD)	See *General Recommendations.*
Edge neutral pressure gauges	None.
Edge Rotation Diagnostics (Ti, VΦ, Vppol)	Replace optics with quartz if darkening is a problem.
Fast camera view of RF antennas	See *General Recommendations.*
Fast ion D-α diagnostic	Check structural supports and strengthen if necessary.
Fast IR Camera	Radiation shielding to reduce noise. See *General Recommendations.*
Fast lost-ion probe (energy/pitch	Reinforce structural supports if necessary.

angle resolving)	
Fast visible camera	See *General Recommendations.*
Fission chamber neutron measurement	None.
Gas-puff Imaging (2msec)-midplane and divertor	Increase magnetic and neutron shielding for electronics. Replace fiber optics with quartz if darkening occurs.
Halo Tile current detectors	Add a conduction path if heat is a problem and if possible. If not, replace with higher-grade materials if possible.
High-n and high-frequency Mirnov arrays	Replace/modify digitizers for new magnetic fields if necessary.
Interferometry/forward scattering (1 mm, 1ch)	Replace G10 base if activation becomes a problem.
IR cameras (30 Hz) (3)	See *General Recommendations.*
Langmuir probe array-inter-LLD	None.
Langmuir probes-outboard edge	None.
Langmuir probes-PFC tiles	None.
Langmuir probes-RF antenna	None.
LLNL EUV spectrometer LoWEUS	None.
LLNL EUV spectrometer XEUS	None.
Locked-mode detectors	Replace/modify digitizers if necessary. Make sure new PF supports do not interfere with sensors.
Magnetics for equilibrium reconstruction	Change mounting scheme if fortafix cannot take extra heat.
Microwave reflectometers (65 GHz backscattering, correlation, FM/CW, fixed frequency)	Reinforce copper pipes with stainless steel as has been done in the past. Replace Teflon cables with other material if degradation becomes a problem.
Midplane tangential bolometer array	None.
Motional Stark Effect based on Collisionally-Induced Fluorescence	Increase shielding to reduce noise. Replace fiber optics with quartz if necessary. Replace G10 parts with other material if activation becomes a problem.
Motional Stark Effect based on Laser-Induced Fluorescence	Increase shielding to reduce noise. Replace fiber optics with quartz if necessary.
Multi-pulse Thomson scattering (30 ch, 60 Hz)	Increase shielding to reduce noise. Add polarizer to reduce noise and saturation problems if necessary. Replace G10 components if activation becomes a problem.
Neutron detectors (2 uranium and 4 fast scintillator)	Add a channel to accommodate higher neutron flux.
P-CHERS: Vθ(r) (75 ch)	Replace optics with quartz if darkening becomes a problem.
Plasma TV	See *General Recommendations.*
RF Antenna (ECH Launcher)	None.
RF edge magnetic probe	None.
RWM Coils	Check mounting.
RWM sensors (n = 1, 2, and 3)	Reinforce for halo current forces. Replace/modify digitizers to prevent saturation.
Sample probe	None.

Scrape-off layer reflectometer	Reinforce with stainless steel if necessary.
SWIFT 2-D flow diagnostic	See *General Recommendations.*
Tile temperature thermocouple array	None.
Ultra-soft x-ray arrays - tomography	Increase shielding to prevent more noise. Replace G10 mounting plate to reduce activation. Add structural support for disruption loads.
UV survey spectrometer (SPRED)	None.
Vertical x-ray crystal spectrometer	None.
Visible (VIPS) survey spectrometer	Replace glass fiber optics with quartz if darkening becomes a problem.
Visible bremsstrahlung detector (1 ch)	Replace window with quartz if darkening becomes a problem.
Visible filterscopes	See *General Recommendations.*
VUV transmission grating spectrometer	Increase structural supports if necessary. If fast cameras are added to diagnostic, see *General Recommendations.*
Wall coupon analysis	Check walls supports.

General Recommendations

If noise becomes a problem for the diagnostic, add electromagnetic and neutron shielding. This should reduce the noise caused by the neutron radiation as well as by the spa's. To prevent wire fatigue in the vessel-mounted diagnostics, adding insulation around the wires may be desired. The windows will need to be cleaned more frequently because there will be a larger amount of deposition after each pulse due to the longer pulse length. Also, as was mentioned above, the holes through the test cell wall should be drilled at angles to prevent radiation from penetrating. For any cameras, if the fiber optics are made of glass and begin to darken too quickly, it may be necessary to replace them with quartz. Also, for any camera that has a silicon chip, the neutron shielding should be increased to prevent the noise from increasing.

For more information regarding any of the diagnostics, please refer to pointer 1 from the List of Pointers in the Appendix.

ANSYS Analysis of Shutters

Solid Modeling and Meshing

For each analysis that is performed, the solid model is imported as an .iges file. The .iges files were also created using ANSYS classic. The model is then sliced in appropriate places so the model can be meshed using bricks instead of tetrahedron. The pieces are then "glued" together to attach the surfaces on adjacent pieces together. The element type used in meshing the solid model for the eddy current analysis is SOLID 97 because of the ease with which vector potentials can be applied. For the thermal analysis, SOLID 70 was used. Bricks are preferred for this element type because it is only an 8-node brick. Also, using bricks allows for creating a mesh that is several elements thick much simpler without creating a very large number of elements. When the initial analysis is done (eddy current or thermal), the model is changed to SOLID 45. Each of the shutter types are shown unmeshed and meshed in the figures below. The relevant drawings for each of these figures can be seen in Table 4 of the Appendix.

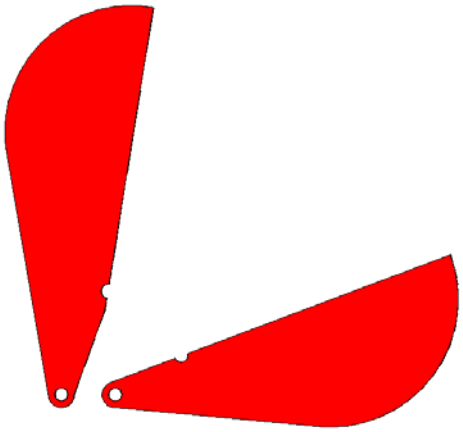

Figure 3. Thomson scattering shutter solid model.

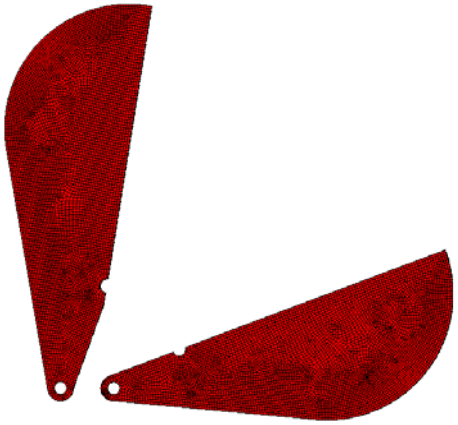

Figure 4. Thomson scattering shutter brick mesh.

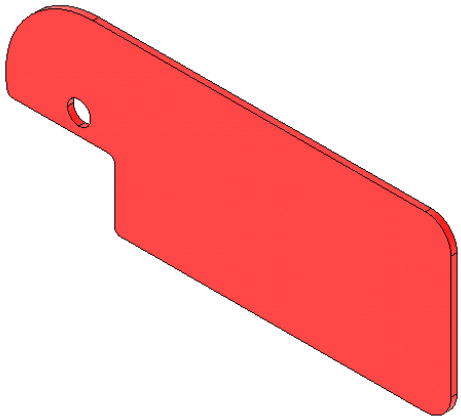

Figure 5. Shutter type 1 solid model.

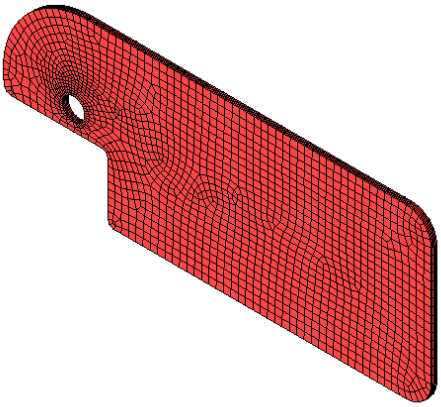

Figure 6. Shutter type 1 brick mesh.

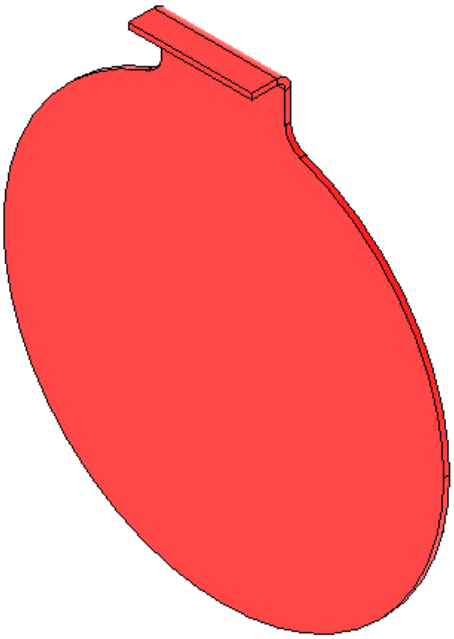

Figure 7. Shutter type 2 solid model.

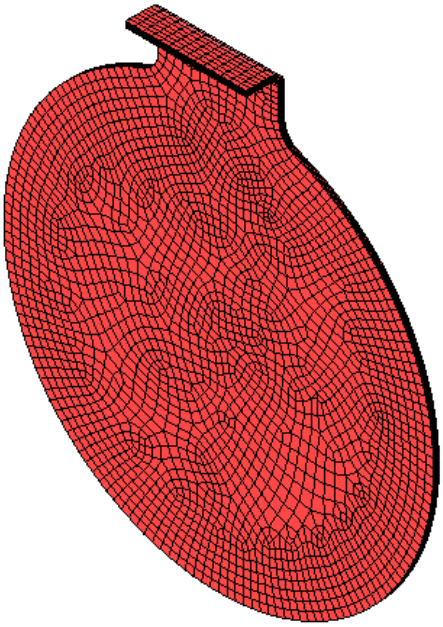

Figure 8. Shutter type 2 brick mesh.

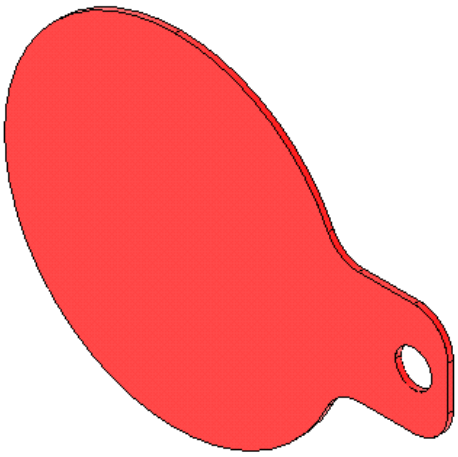

Figure 9. Shutter type 3 solid model.

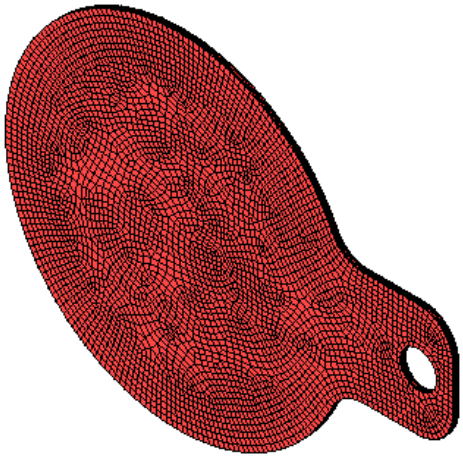

Figure 10. Shutter type 3 brick mesh.

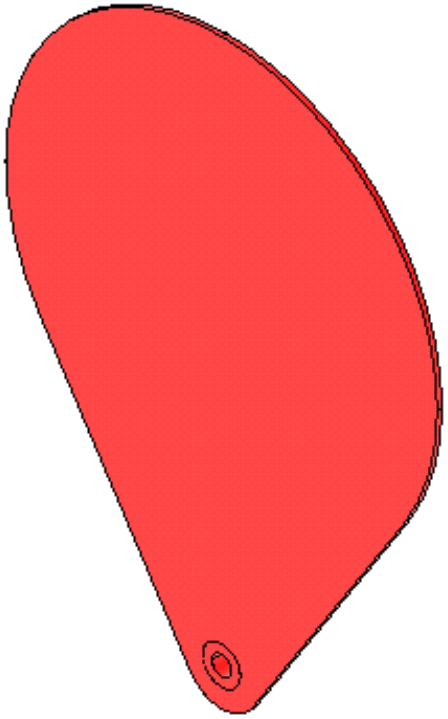

Figure 11. Shutter type 4 solid model.

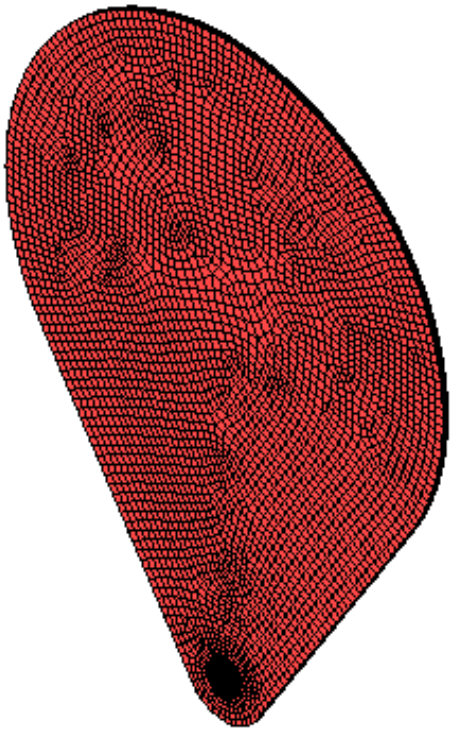

Figure 12. Shutter type 4 brick mesh.

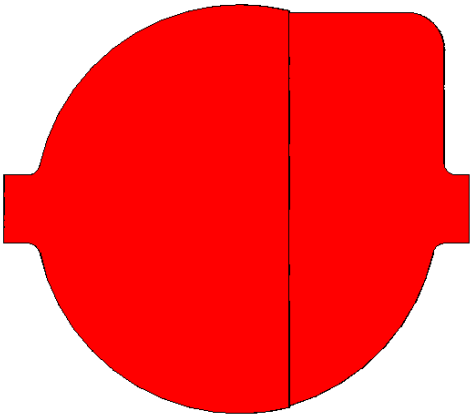

Figure 13. Shutter type 5 solid model.

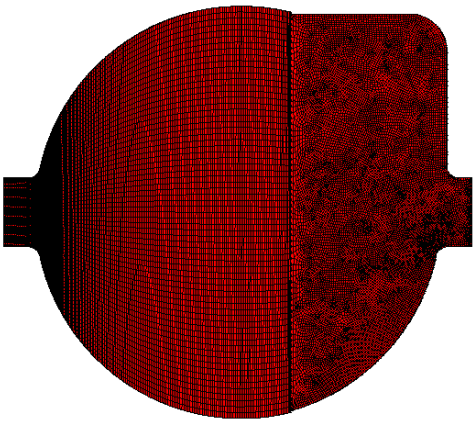

Figure 14. Shutter type 5 brick mesh.

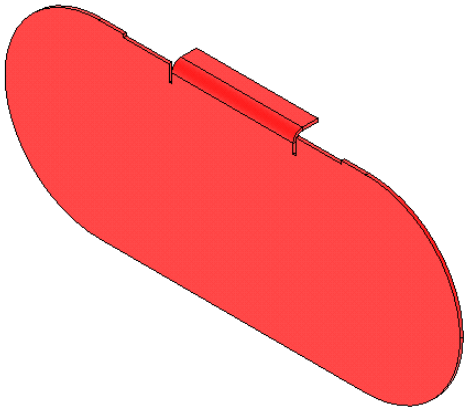

Figure 15. Shutter type 6 solid model.

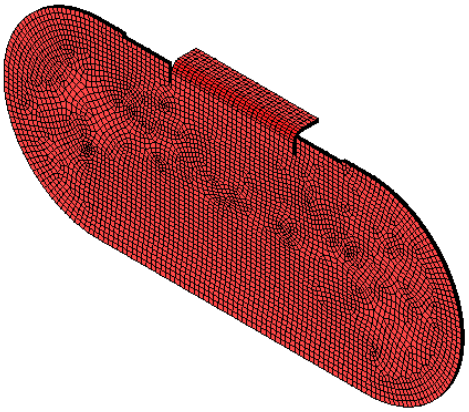

Figure 16. Shutter type 6 brick mesh.

ANSYS Eddy Current Analysis

After the models had been successfully meshed, two sets of vector potentials were imposed on them at different time steps to simulate a change in the magnetic field. Rather than simulating a full disruption as has been done in the past, a known final magnetic field and change in magnetic field was applied. The magnetic field data was mapped using a script written in Matlab and was applied to a table format, where the user could choose a specific location, as well as to a heat map format, where the user could look an image of the cross section of NSTX and estimate the fields and field changes of interest for this purpose.

The vector potentials were imposed throughout the shutter in order to calculate the resistive solution to the problem. The resistive solution was used since it is the most mechanically demanding solution because the eddy currents, and therefore the forces on the shutter, have fully developed. A Volt degree of freedom was applied to the node with the lowest value (normally 1) as a reference point for the model. This reference point is arbitrary, as there is no ground for these models. In all of the shutters, eddy currents developed in an expected pattern (following the boundary of the model). Several hand calculations were performed and compared to the ANSYS-calculated solution as a check.

Thomson Scattering Shutter

The Thomson scattering shutter was analyzed in a “constrained” configuration and an “unconstrained” configuration. As can be seen below, the constrained configuration holds the shutter plates at their pin holes as well as at a section along the shutter while the unconstrained configuration holds the shutter plates only at their pin holes.

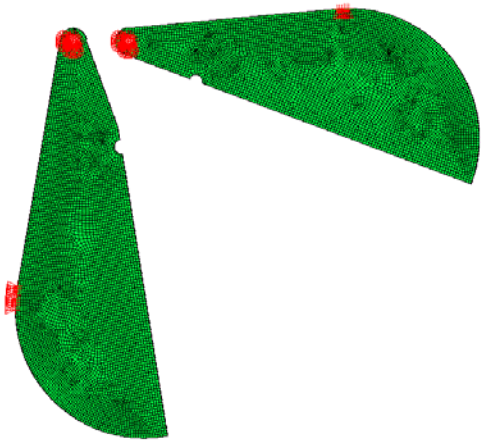

Figure 17. Thomson scattering shutter in constrained configuration.

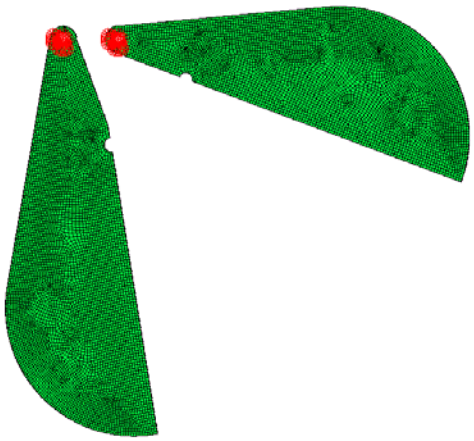

Figure 18. Thomson scattering shutter in unconstrained configuration.

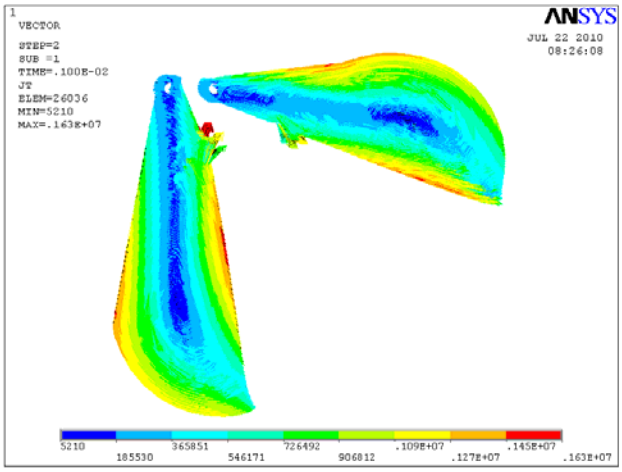

Figure 19. Eddy currents due to magnetic field change from disruption.

The eddy currents in the shutter developed in the expected manner, they followed the edge of the shutter with the largest current densities at the edge. The figure to the left shows the currents that developed in the shutters. These eddy currents are the same for the constrained and unconstrained configuration since the Volt constraint is arbitrary. The figures below show the stresses that developed due to these eddy currents. From the images, it is clear that the two different configurations have developed vastly different stresses.

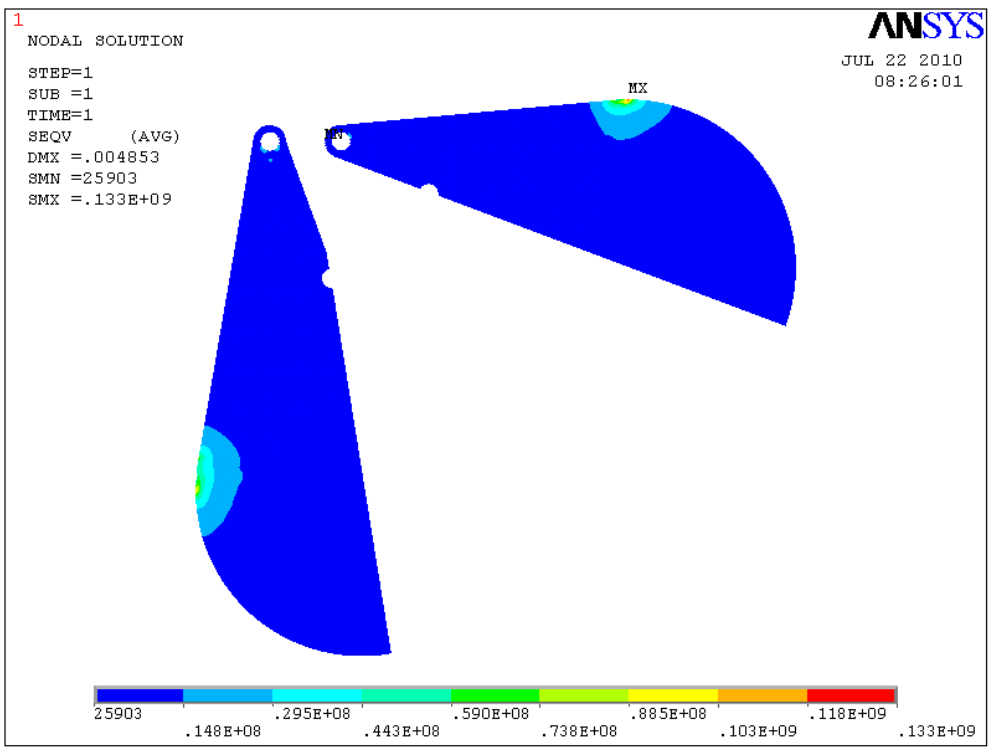

Figure 20. Von Mises stresses that develop in the constrained Thomson scattering shutter due to worst-case disruption. Maximum stress (ignoring singular values): 90 MPa

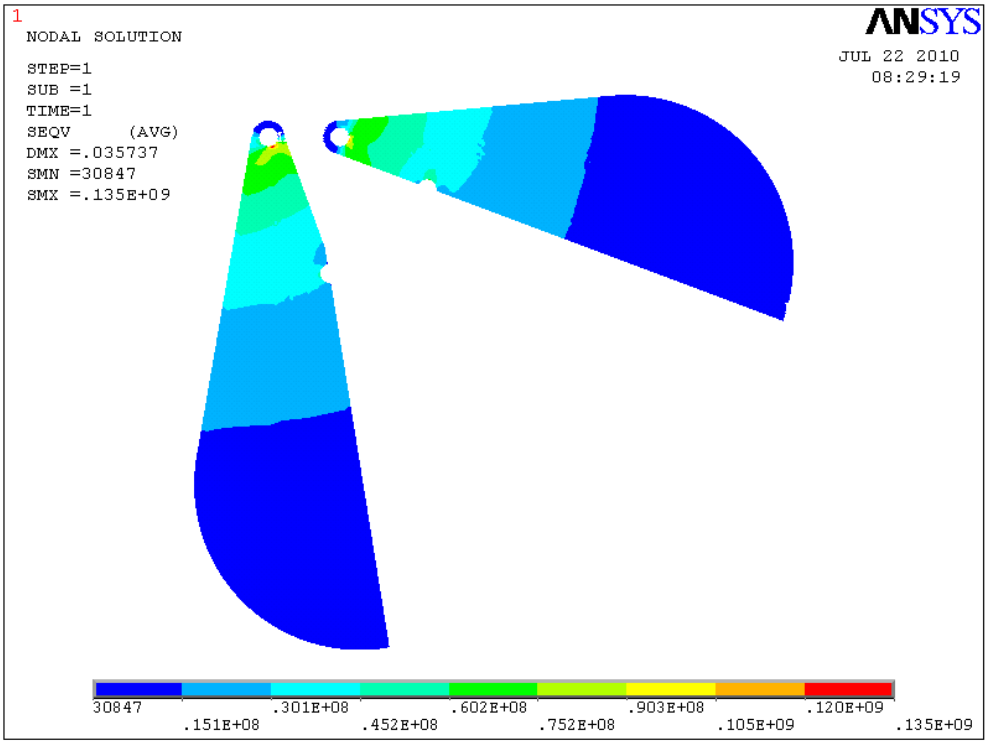

Figure 21. Von Mises stresses that develop in the unconstrained Thomson scattering shutter due to the worst case disruption. Maximum stress (ignoring Singular values): 90 MPa

The maximum stresses that develop in this shutter in both cases are compressive, caused by the hardware used to constrain the shutter. Maximum stress calculated by ANSYS is near 135 MPa in both cases. However, this maximum is also only at a single node and is most likely due to an over-constrained model. Ignoring this node, the maximum stress in both cases is approximately 90 MPa. Unfortunately, the titanium alloy used for this shutter is not known. For the lowest grade titanium (grade 1), the compressive yield strength of the material is estimated to be 170 MPa. For higher grade titanium alloys, the compressive yield strength can be as high as 970 MPa. Therefore, the stresses are deemed to be allowable. If the titanium alloy used is grade 1, I recommend upgrading to at least grade 2 if necessary, as it has very similar mechanical properties but yield stresses near 300 MPa.

In the case of the unconstrained configuration, the deflection of the shutter could allow foreign material to be deposited on the window or lens used in the Thomson scattering diagnostic. The maximum deflection is more than 3.5 cm. This will only be a problem if the shutter is not properly held during a disruption while the shutter is closed. Since the shutter is normally open during a disruption, this worry can be neglected. If the large deflection is a problem, adding reinforcement to the shutter may be desired.

Shutter Type 1

Shutter Type 1 was analyzed using two different locations: at midplane and at the location of a vertical port in the divertor. The eddy currents, below, are similar in pattern, but the magnitudes are vastly different, was expected.

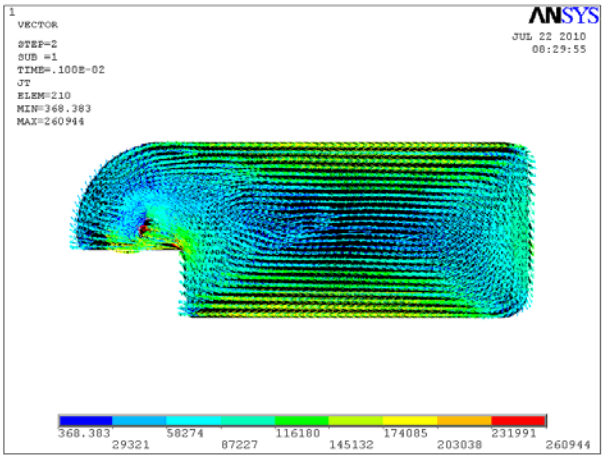

Figure 22. Eddy currents in shutter type 1 when placed at midplane.

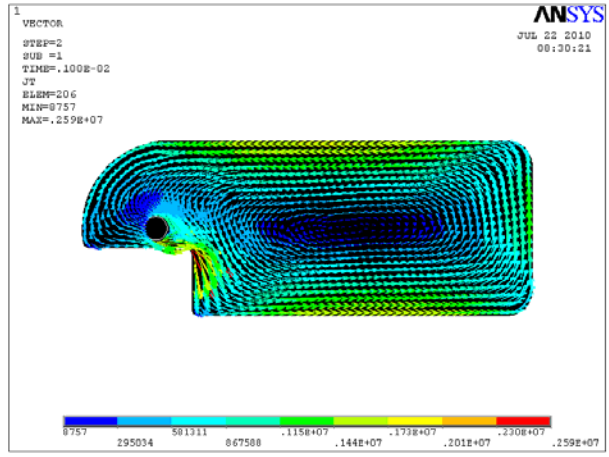

Figure 23. Eddy currents in shutter type 1 when placed at vertical port in the divertor, facing upward.

The magnitudes of the eddy currents are very close to those found using a simplified hand calculation. The figures below show the stresses that develop due to these eddy currents.

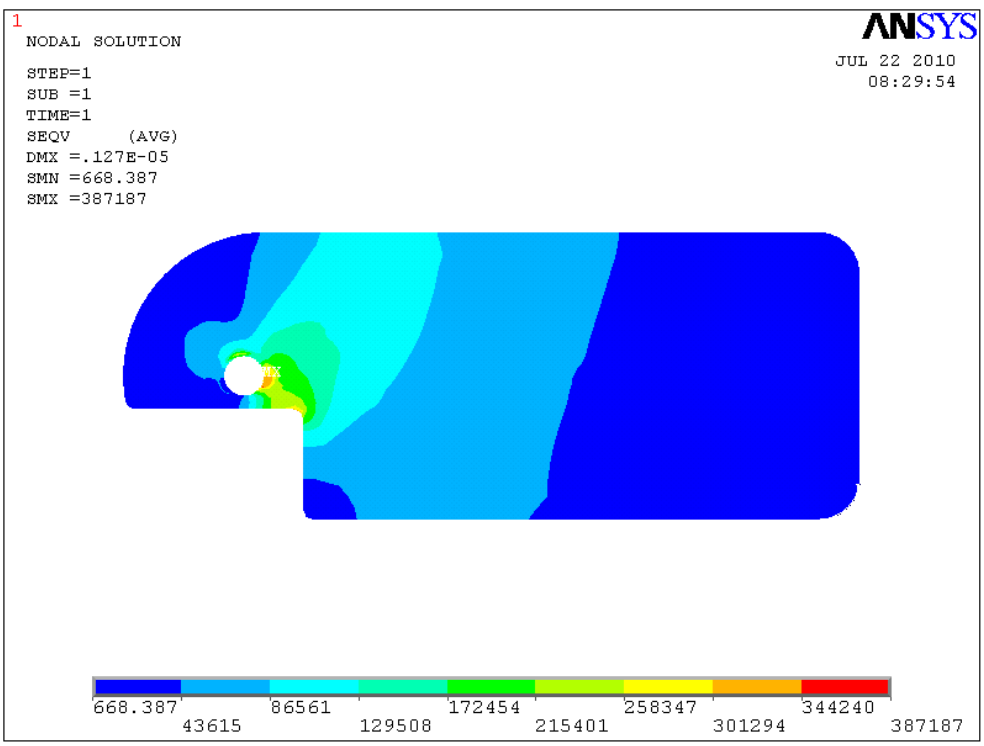

Figure 24. Von Mises stresses that develop in the type 1 shutter due to the worst case disruption when placed at midplane. Maximum stress: 0.39 MPa

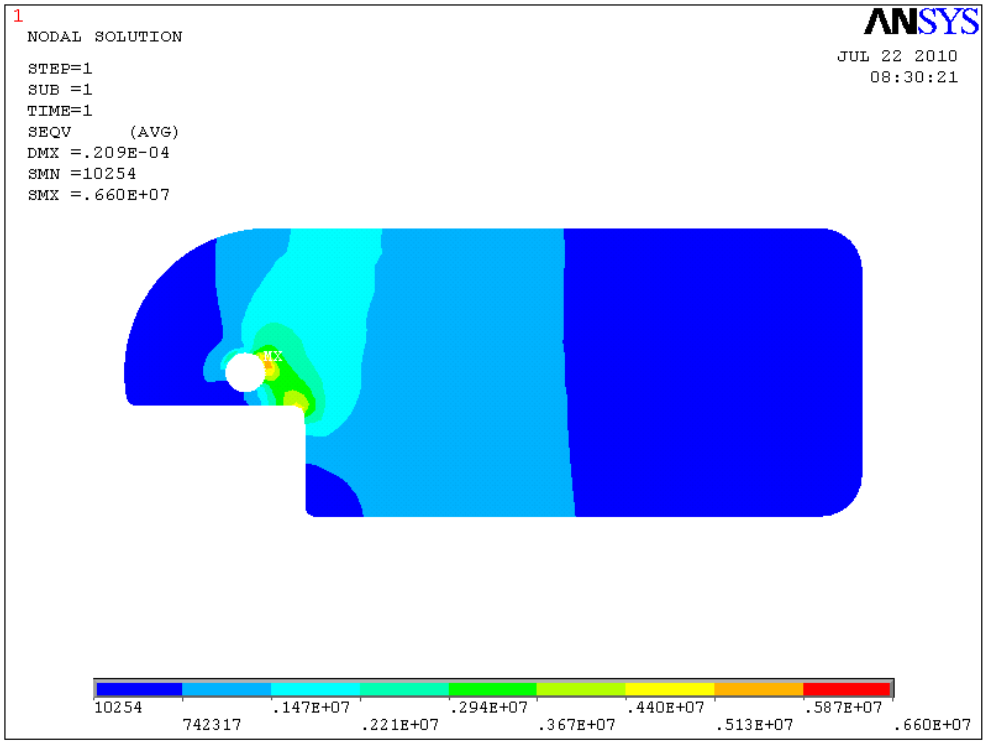

Figure 25. Von Mises stresses that develop in the type 1 shutter due to the worst case disruption when placed at a vertical port in the divertor. Maximum stress: 6.60 MPa

Shutter type 1 is made from 304 Stainless Steel. The allowable stresses of all types are well-above the maximum calculated value of 6.60 MPa. Therefore, these shutters should be unaffected by the NSTX-CSU.

Shutter Type 2

Shutter type 2 was analyzed at two different locations in both an open and a closed position. The locations used were midplane and approximately 0.5 meters below midplane at a radius near the passive plates. The shutter was analyzed in both the open and closed positions because these positions change the angle of the shutter by 90 degrees, creating vastly different eddy currents. The eddy currents that developed are in the figures below. They are consistent with the simplified hand calculations.

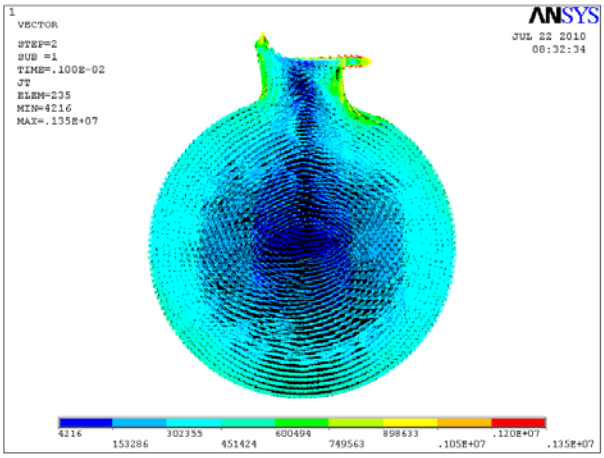

Figure 26. Eddy currents in shutter type 2 when placed at midplane in the closed position.

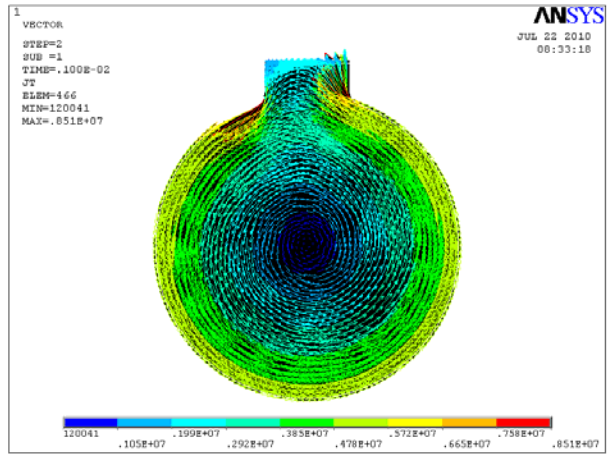

Figure 27. Eddy currents in shutter type 2 when placed at midplane in the open position.

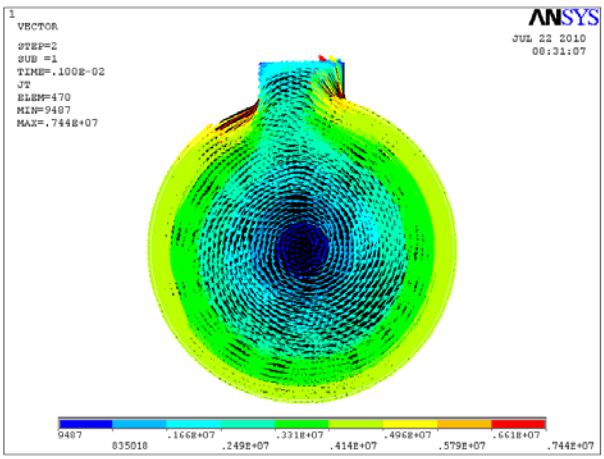

Figure 28. Eddy currents in shutter type 2 when placed 0.5 meters below midplane near the passive plates in the open position.

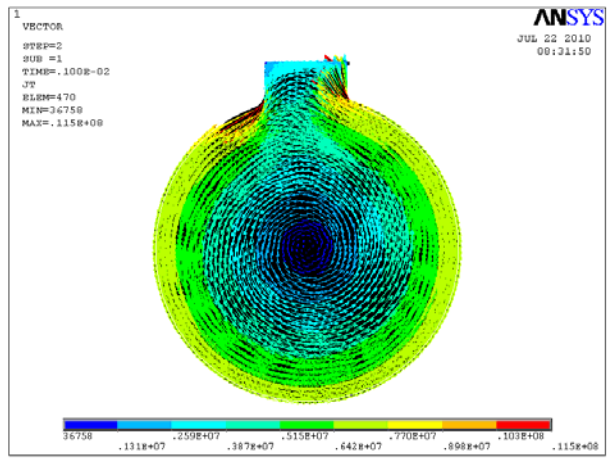

Figure 29. Eddy currents in shutter type 2 when placed 0.5 meters below midplane near the passive plates in the closed position.

Like the eddy currents, the stresses that develop are also very different in magnitude, though they are approximately the same in the way that they developed. The von Mises stresses that developed due to these eddy currents are below.

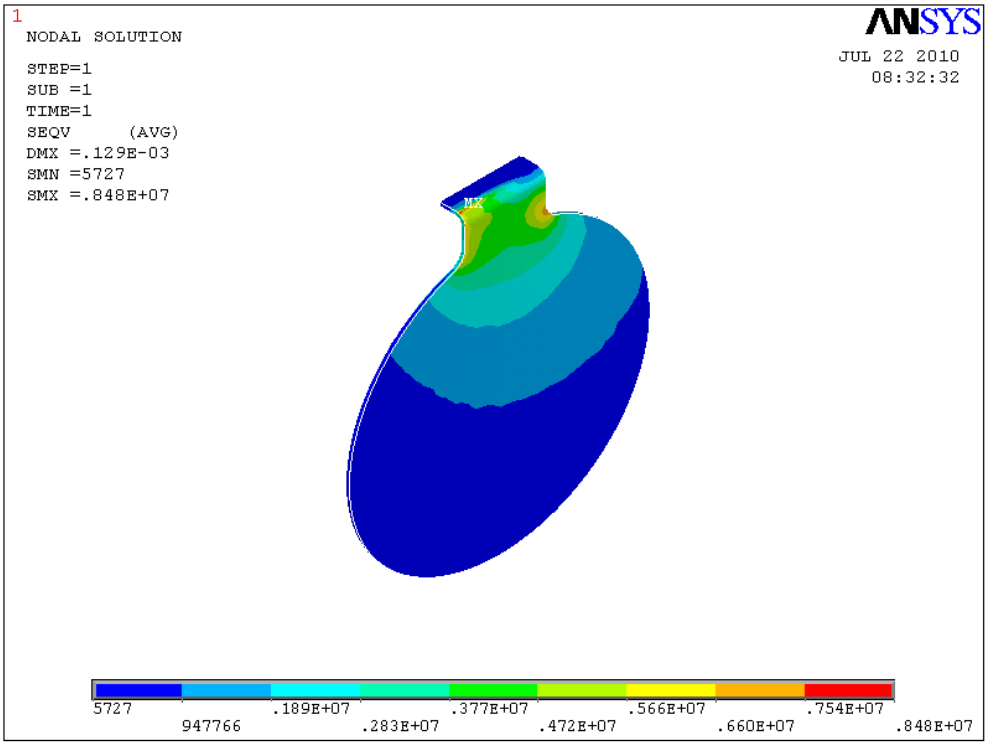

Figure 30. Von Mises stresses that develop in the type 2 shutter due to the worst case disruption when placed at a midplane in the closed position. Maximum stress: 8.5 MPa

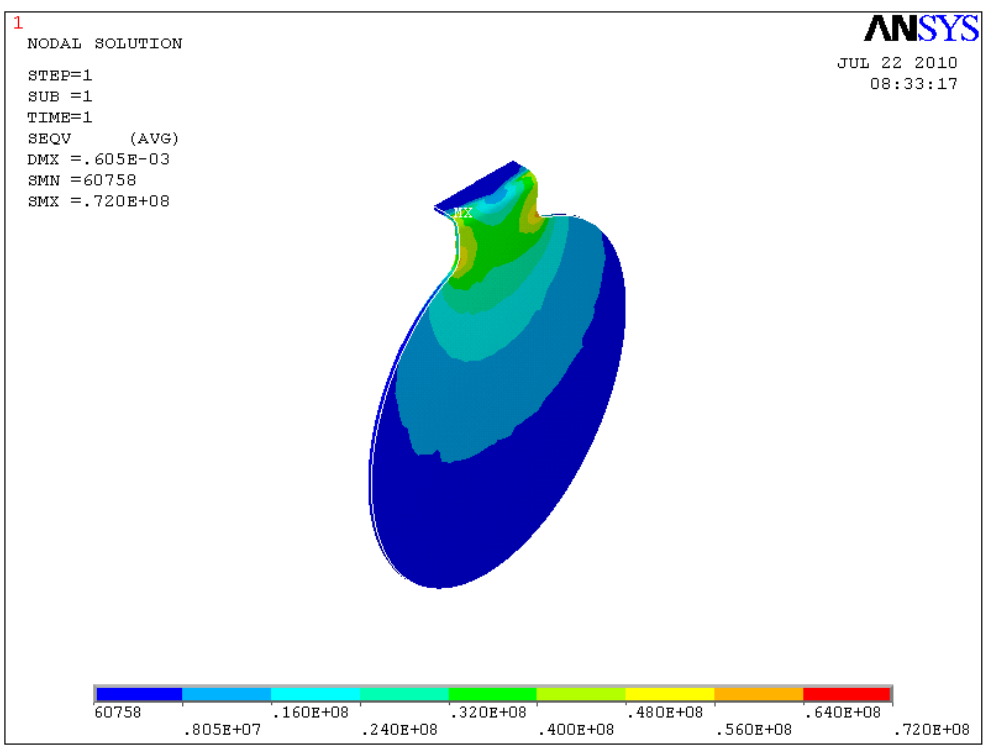

Figure 31. Von Mises stresses that develop in the type 2 shutter due to the worst case disruption when placed at a midplane in the open position. Maximum stress: 72.0 MPa

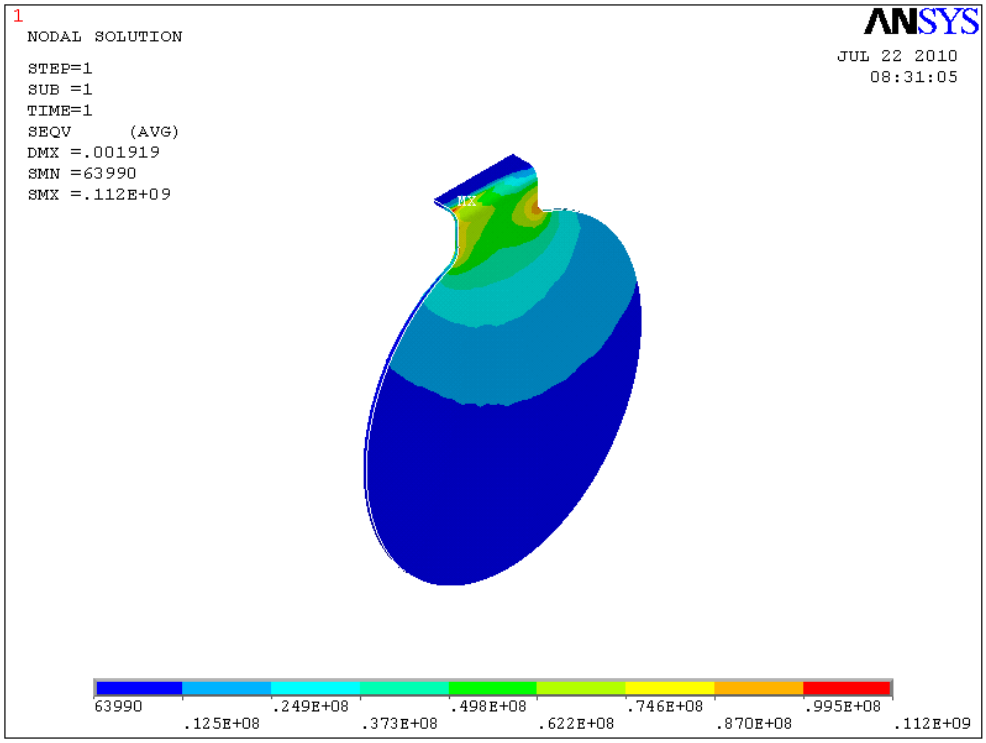

Figure 32. Von Mises stresses that develop in the type 2 shutter due to the worst case disruption when placed 0.5 meters below midplane near the passive plates in the closed position. Maximum stress: 112 MPa

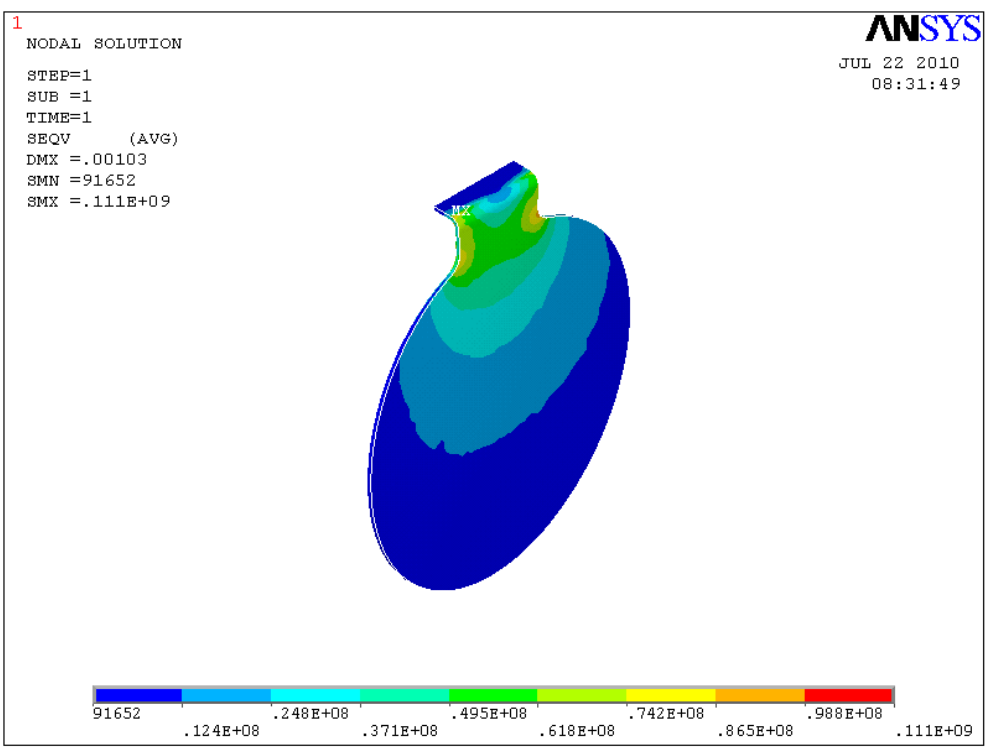

Figure 33. Von Mises stresses that develop in the type 2 shutter due to the worst case disruption when placed 0.5 meters below midplane near the passive plates in the open position. Maximum stress: 111 MPa

For these shutters, the primary stress is in compression and tension which have yield strengths of 210 MPa and 290 MPa, respectively. The tensile and compressive stresses have magnitudes near 95 MPa (in the worst case), which is well-below the yield strength. Also, the maximum shear stress in the worst case is near 55 MPa, which is well below the shear strength of 110 MPa. The maximum deflection in the shutter is less than 2 mm in all cases, which should not affect their functionality.

Shutter Type 3

Shutter type 3 was analyzed at three different locations: at midplane, 0.35 meters below midplane at the vacuum vessel wall, and in a vertical bay in the divertor. The eddy currents that developed at each of these locations are below. They are consistent with the simplified hand calculations.

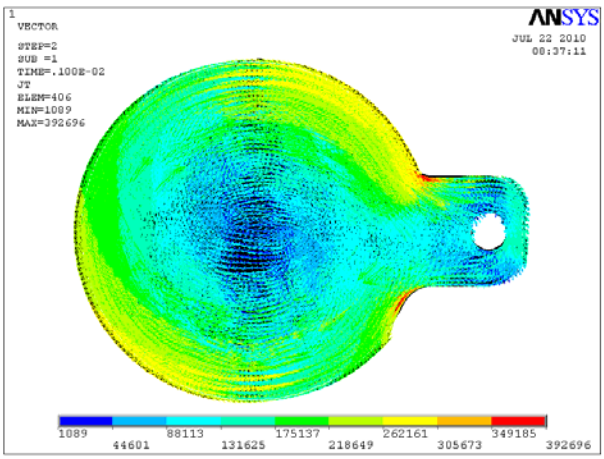

Figure 34. Eddy currents in shutter type 3 when placed at midplane.

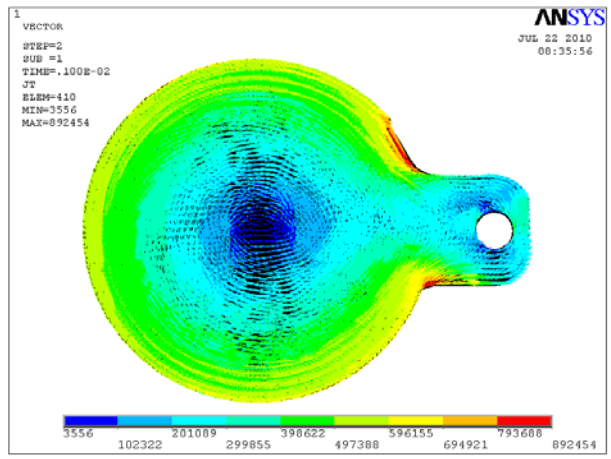

Figure 35. Eddy currents in shutter type 3 when placed 0.35 meters below midplane at the vacuum vessel wall.

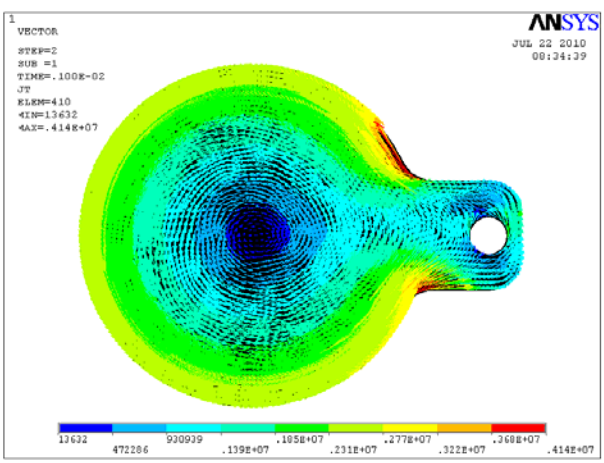

Figure 36. Eddy currents in shutter type 3 when placed in a vertical bay in the divertor, facing upward.

Using these eddy currents, the stresses in the figures below were calculated.

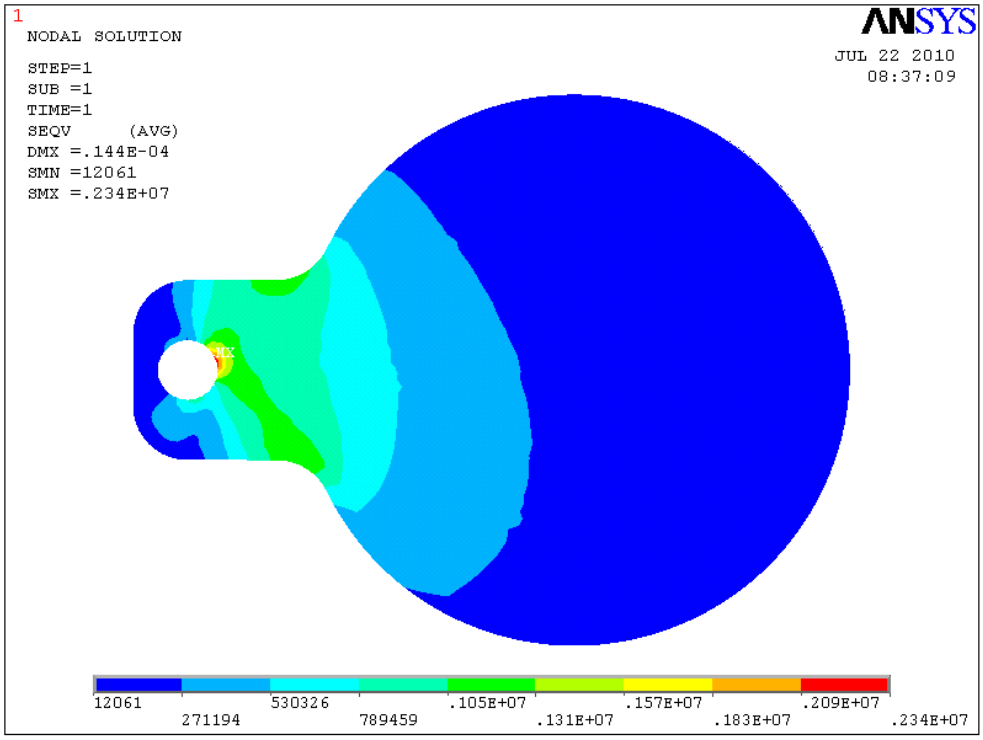

Figure 37. Von Mises stresses that develop in the type 3 shutter due to the worst case disruption when placed at a midplane. Maximum stress: 2.34 MPa

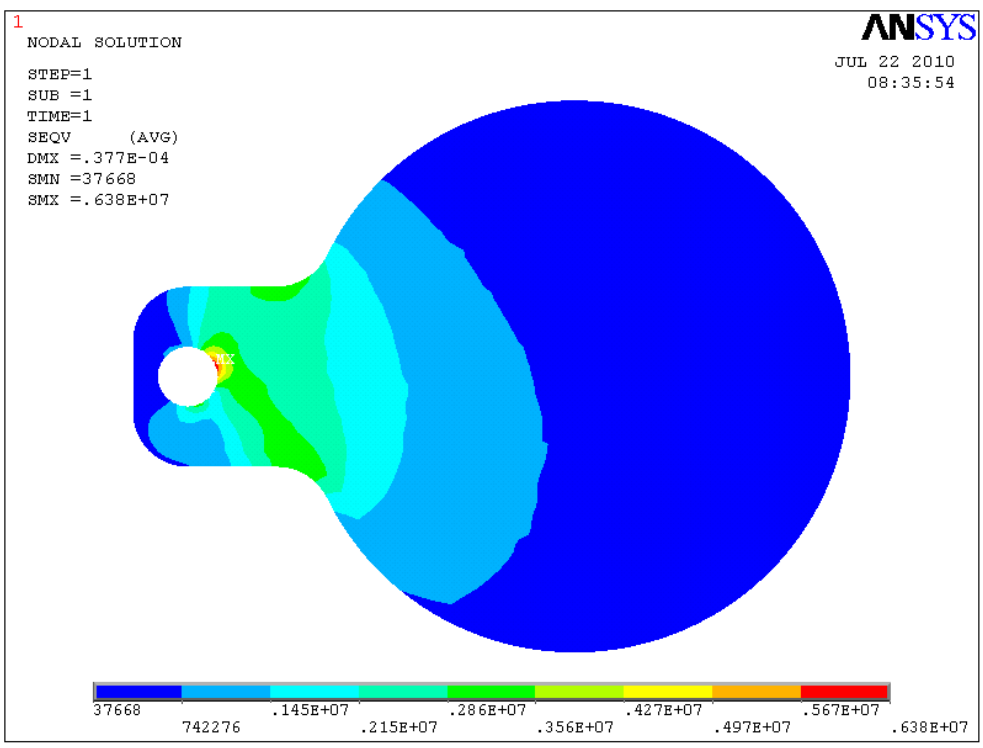

Figure 38. Von Mises stresses that develop in the type 3 shutter due to the worst case disruption when placed 0.35 meters below midplane near the vacuum vessel wall. Maximum stress: 6.38 MPa

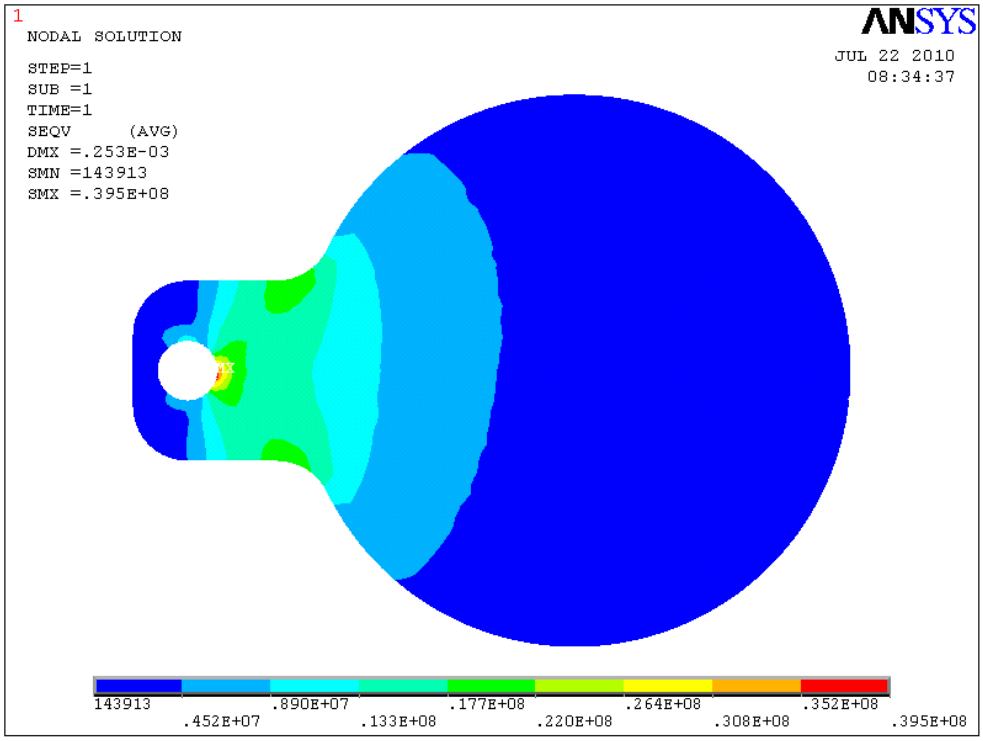

Figure 39. Von Mises stresses that develop in the type 3 shutter due to the worst case disruption when placed in a vertical bay in the divertor. Maximum stress: 39.5 MPa

Since shutter type 3 is made of stainless steel, the stresses are well-below the yield stresses and are allowable. The primary stresses are in compression and tension which have yield strengths of 210 MPa and 290 MPa, respectively. The maximum shear stresses are also all below 10 MPa, which is well below the shear strength of 110 MPa. The deflections in these shutters are all less than 0.5 mm, so the deflection should not reduce the functionality of the shutter.

Shutter Type 4

Shutter type 4 was analyzed at only one location: at a vertical bay in the divertor. The eddy currents that developed in the shutter at this location are below. They are consistent with the simplified hand calculations.

Using these eddy currents, the stresses in the figure below were calculated.

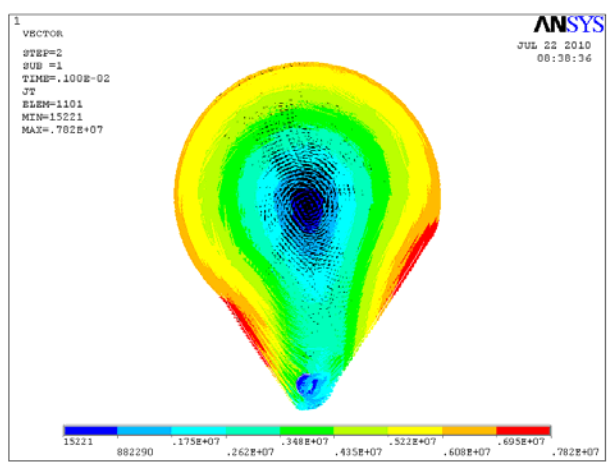

Figure 40. Eddy currents in shutter type 4 when placed in a vertical bay in the divertor, facing upward.

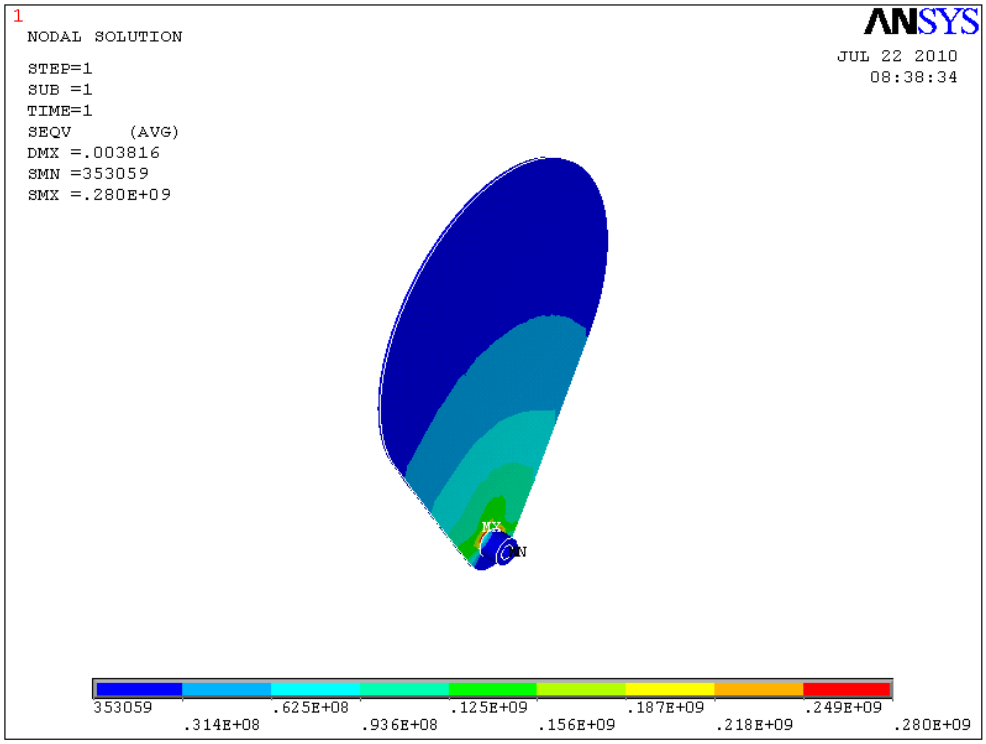

Figure 41. Von Mises stresses that develop in the type 4 shutter due to the worst case disruption when placed in a vertical bay in the divertor. Maximum stress (ignoring sharp corners): 160 MPa

The maximum stress found in this shutter (ignoring the sharp corners) is approximately 160 MPa. This stress is below the yield stress for the material (304 stainless steel), but it is approaching the compressive strength. If the shutter begins to fail, my recommendation is to use a material with a higher electrical resistivity, such as Inconel 625. Inconel 625 is also a much stronger material than 304 stainless steel.

Shutter Type 5

Shutter type 5 was analyzed at only one location: at midplane. The eddy currents that developed in the shutter at this location are to the right. They are consistent with the simplified hand calculations.

Using these eddy currents, the stresses in the figure below were calculated.

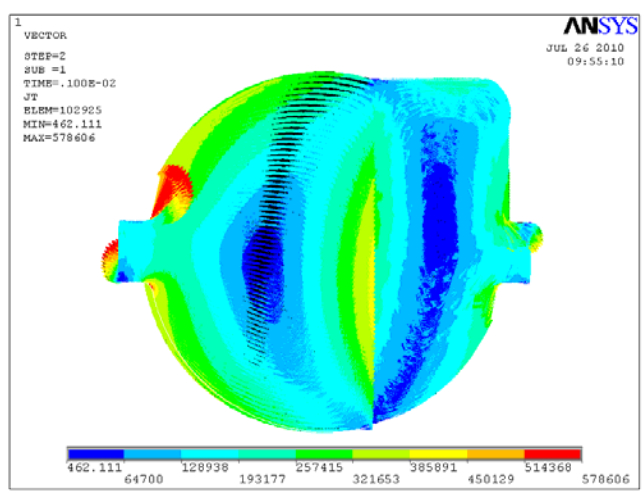

Figure 42. Eddy currents in shutter type 5 when placed at midplane.

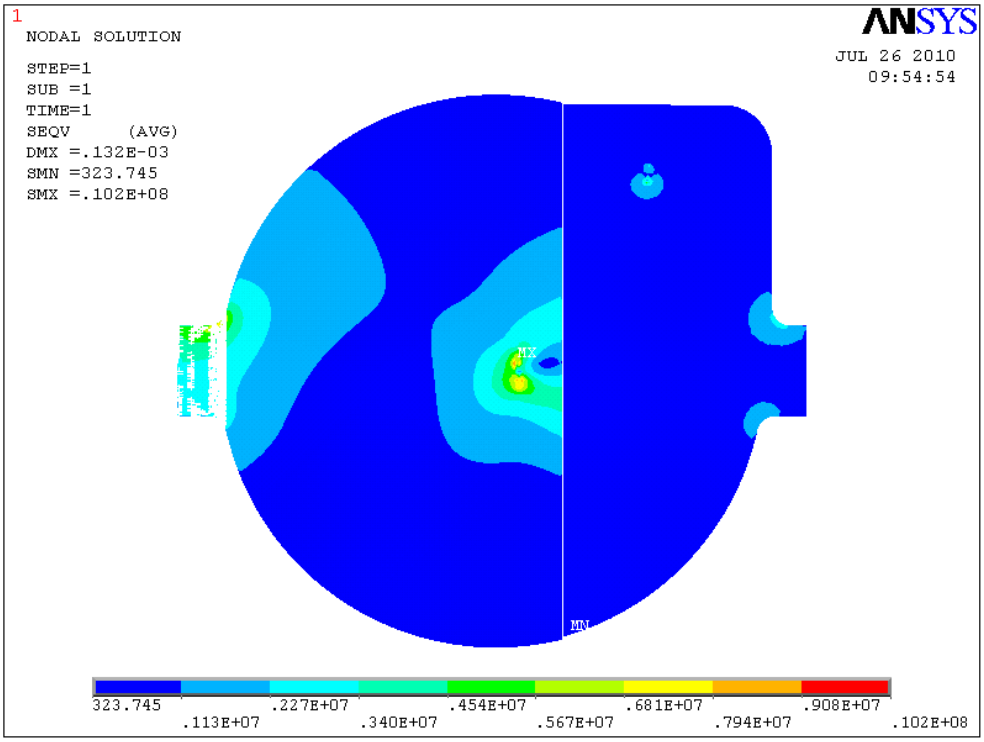

Figure 43. Von Mises stresses that develop in the type 5 shutter due to the worst case disruption when placed at midplane. Maximum stress: 10.2 MPa

The maximum stress found in this shutter is approximately 10.2 MPa. This stress is concentrated around a section that is constrained radially. It is also well-below the yield stress of Inconel 625. The deflection in the shutter is also very small (less than 0.5 mm) and should not affect the functionality of the shutter. Therefore, this shutter should be unaffected by the NSTX-CSU.

Shutter Type 6

Shutter type 6 was analyzed at only one location: at a vertical bay in the divertor. This shutter was analyzed in both the open and closed positions. The eddy currents that developed in the shutter at this location are below. They are consistent with the simplified hand calculations.

Using these eddy currents, the stresses in the figures below were calculated.

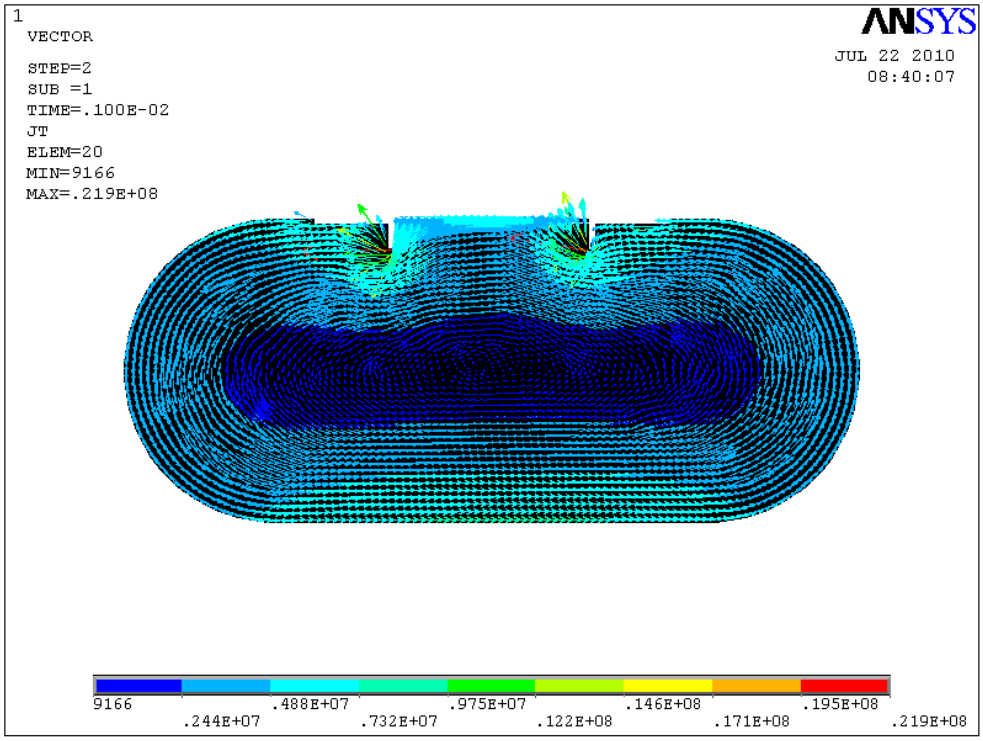

Figure 44. Eddy currents in shutter type 6 when placed in a vertical bay in the divertor in closed position.

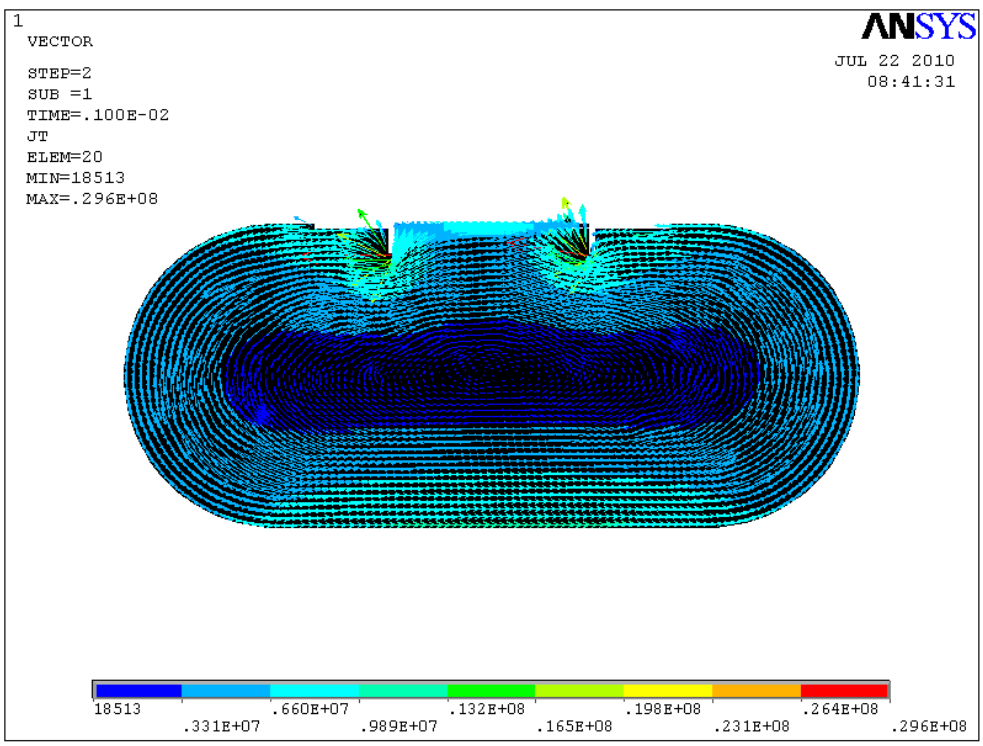

Figure 45. Eddy currents in shutter type 4 when placed in a vertical bay in the divertor in open position.

Using these eddy currents, the stresses in the figures below were calculated.

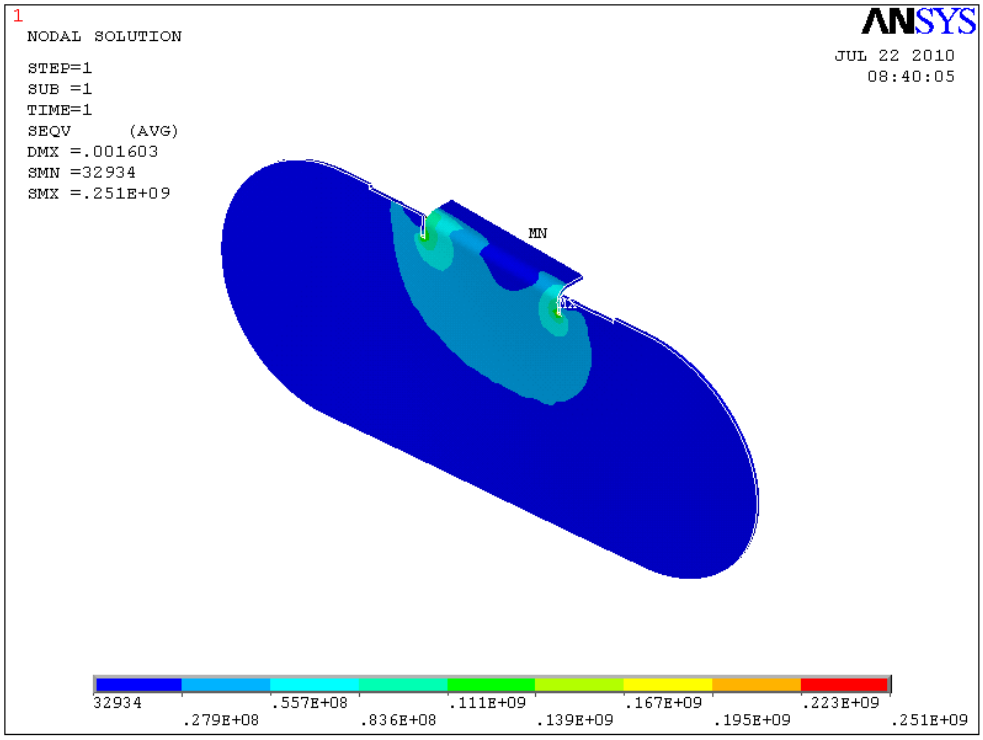

Figure 46. von Mises stresses that develop in the type 6 shutter due to the worst case disruption when placed in a vertical bay in the divertor in the closed position. Maximum stress (ignoring sharp corners): 125 MPa

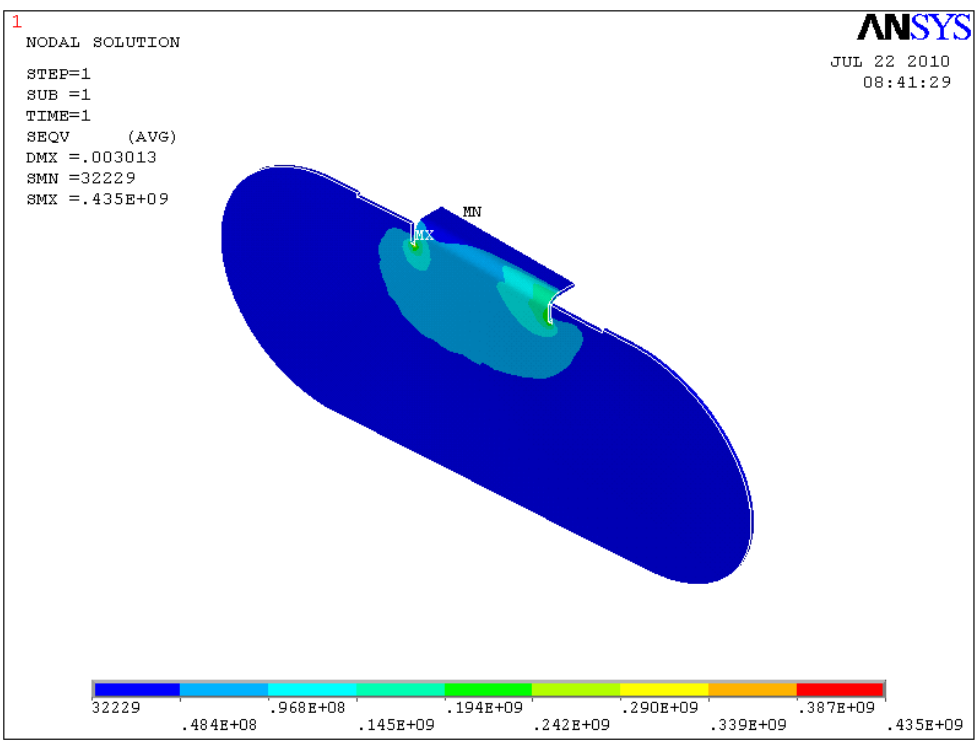

Figure 47. von Mises stresses that develop in the type 6 shutter due to the worst case disruption when placed in a vertical bay in the divertor in the open position. Maximum stress (ignoring sharp corners): 240 MPa

The stresses that develop when the shutter is in the open position appear to be very high. Upon further investigation, I found that the stresses are primarily in tension and compression. The individual stress components are generally smaller than 200 MPa in magnitude. Despite being below the tensile and compressive yield strengths of the material, it may be necessary to replace these shutters with a stronger material with a larger electrical resistivity, such as Inconel 625.

General Recommendations

For any shutters that are in danger of failing or that unexpectedly fail, the use of a stronger material with a higher electrical resistivity may be a solution. The stresses that develop in the shutters due to eddy currents are inversely proportional to the electrical resistivity of the material used (e.g., doubling the resistivity lowers the stress by half). Inconel 625 was recommended above because it has an electrical resistivity of 1.29 μΩ·m, which is 1.8 times larger than the resistivity of stainless steel (72 μΩ·cm). It also has a yield strength (517 MPa) that is approximately 1.8 times larger than that of stainless steel (290 MPa).

For shutters at the midplane, if the stresses due to disruptions are too large, it is likely because the shutter is open with the face of the shutter pointing upward. Changing the shutter geometry so the face points toward the vacuum vessel wall while the shutter is open could fix this problem.

The analyses performed above should be the worst case stresses due to a disruption. The analyses assume that the eddy currents have fully developed, regardless of size or shape. Also, background fields and changes in magnetic field used were the worst known cases at each location. They may be seen in Table 4 of the Appendix.

ANSYS Thermal Analysis

After the solid models have been meshed using SOLID 70, a heat flux is applied to the front face of each shutter. The heat flux is applied for a five second interval since that will be the pulse length of after the upgrade. After the heating calculation is completed, the model is converted into a structural model, where the calculated temperature loads are read into the model. The stresses in the shutters are generally very small (with a few exceptions), as they are mostly free to expand even when constrained. The deflections in the shutters "clam-shelling" were also very small. Clam-shelling is when the edges of a piece of hardware appear to curl toward the center so the maximum deflection would be normal to the plane of the shutter. A sample deflection distribution can be seen to the right. In the sample, the pin hole is held constant and the shutter begins to normal to its surface. A table of results for each of the shutters is below.

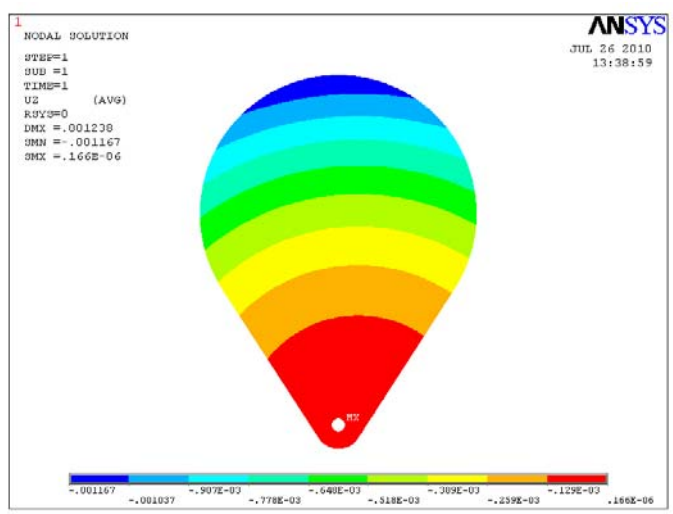

Figure 48. Sample deflection distribution for a curling shutter.

Table 3. Maximum deflections in shutters due to thermal loading.

Shutter Name	Max x-direction deflection (mm)	Max y-direction deflection (mm)	Max z-direction deflection (mm)	Max net deflection (mm)
Thomson	0.88	1.00	2.71	2.89
Type 1	0.23	0.096	0.022	0.24
Type 2	0.18	0.32	0.77	0.83
Type 3	0.26	0.14	0.16	0.31
Type 4	0.19	0.42	1.17	1.24
Type 5	0.51	0.72	0.50	0.82
Type 6	0.34	0.22	0.63	0.73

All of the deflections in the table above are very small (less than 3 mm) and should not affect the operation of the shutters. The stresses that were found were very small, with the exception of those in shutter type 4. In shutter type 4, the maximum von Mises stress (ignoring sharp corners and nodal constraints) was near 40 MPa. However, the location of this high stress region should not increase the cumulative stress (added thermal and eddy-current-induced stresses) in the shutter beyond the yield. The maximum thermal stress is located inside the pin hole while the maximum eddy-current-induced stress is located near the boundary of the pinhole and the main section of the shutter.

If thermal deflections become a problem for the shutter of interest, I recommend choosing a new material with a larger thermal conductivity and/or choosing a new material with a higher thermal conductivity so the heat transmits through the material and equilibrates more quickly.

Python Ratcheting Analysis

For a further analysis of the shutters, a ratcheting analysis was done for each shutter type. In this analysis, the shutters are subjected to a heat flux of 0.13 MW/m^2 for fifteen five-second pulses with a cool-down time of fifteen minutes between pulses. For the heating of the shutters, the script uses a modification of the basic heat formula (1), where h is the heat flux, c is the specific heat of the material, ρ is the density of the material, t_s is the thickness of the shutter, dT is the change in temperature (in Kelvins), and dt is the change in time. For the cooling of the shutter, it uses radiative cooling.

$$dT = \frac{h \cdot dt}{c \cdot \rho \cdot t_s} \qquad (1)$$

For each run, the script will output a ratcheting graph, like the one seen to the right, as well as specific information about the run. The information output to the terminal includes the parameters input by the user as well as the temperature after a single pulse and the maximum ratcheted temperature, both in °C. The graph to the right is taken from a run for a 1 mm thick shutter made of 304 stainless steel. The temperature after the first pulse was 181 °C and the

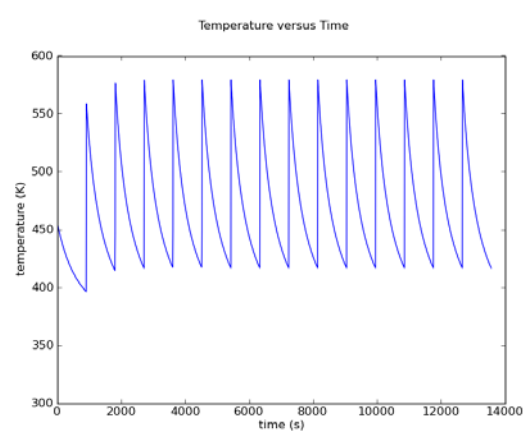

Figure 49. Sample ratcheting graph from Python script.

ratcheted temperature was 306 °C. The plot below shows the results over a range of thicknesses from 0.1 mm to 5 mm for shutters made from Inconel 625 and 304 stainless steel.

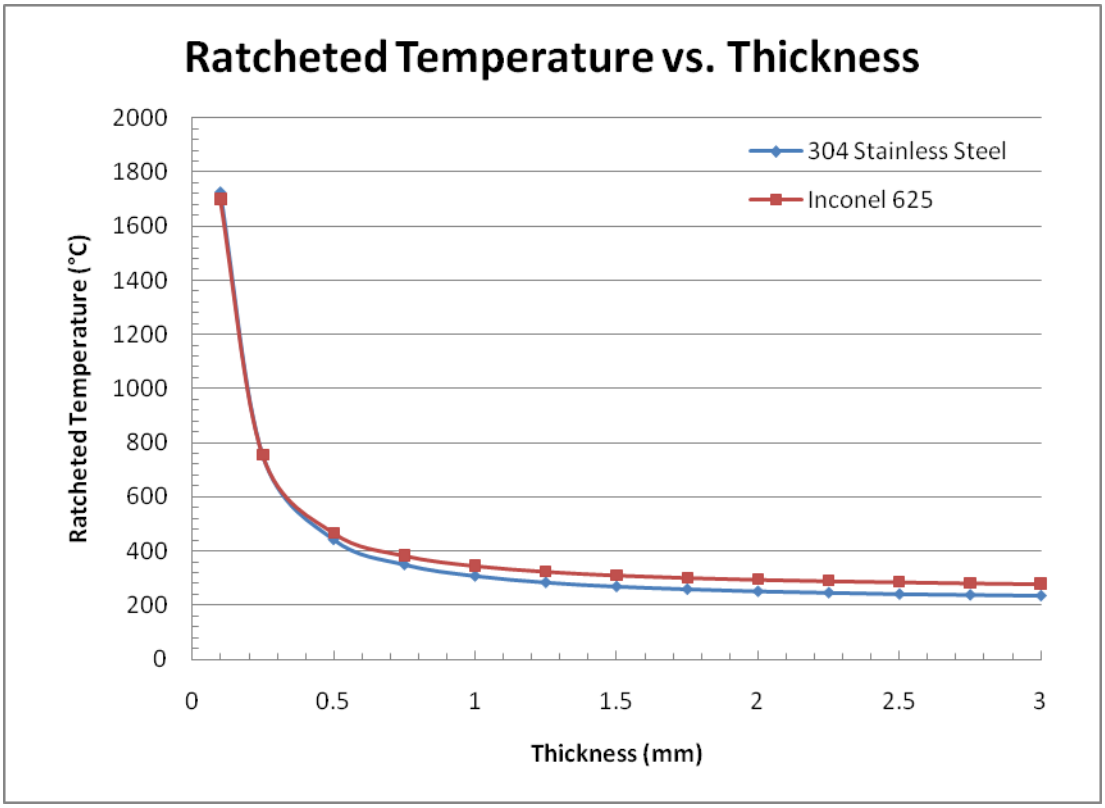

Figure 50. Maximum ratcheted temperature vs. shutter thickness for shutters ranging from 0.1 to 3.0 mm.

The thinnest shutter analyzed in this analysis has thickness of 0.03", or 0.762 mm. As can be seen above, the ratcheted temperature of this shutter is near 400 °C. This value is well below the annealing temperatures of both 304 stainless steel and Inconel 625, which are either near or above 900 °C.

Scripts and Macros

Below are some of the scripts and macros that were used to perform these analyses.

ANSYS Eddy Current Analysis Macro

The macro below is a single version of the eddy current analysis macro. There are several versions with slight modifications so the script is applicable to the specific situation of interest. The macro below also calls other macros, which will be shown if relevant or just simply described.

```
fini
/clear
jobid = 'type2'

/filname,%jobid%_em
/aux15
igesin,jobid,iges
/auto
/replot

/prep7
! Material Properties
et,1,97,1
mp,dens,1,8000
mp,murx,1,1.
mp,rsvx,1,720e-9
mp,ex,1,193e9
mp,prxy,1,0.3

/input,'bdots\mesh',txt
bdotx = 0. ! Toroidal
bdoty = 10.      ! Radial
bdotz = -125.    ! Poloidal

bx = 0.55  ! Toroidal
by = -0.02 ! Radial
bz = -0.40 ! Poloidal

!!!!!!!!!!!!!!!!!!!!!!!!!!!!!!!!!!!!!!!!!!!!!!!!!!!!!!!!!!!!!!!!!!!!!!
!Ramp Time
tim = 0.001

allsel
fini

/solu
antype,trans,new
timint,off
```

```
time,0.000001

bx0 = bx - bdotx*tim
by0 = by - bdoty*tim
bz0 = bz - bdotz*tim

nall
'Bdots\b_mac',bx0,by0,bz0
allsel
solve

timint,on
time,tim
outres,all,all
autots,on
nall
'Bdots\b_mac',bx,by,bz
*get,n0,node,,num,min
d,n0,volt,0
allsel
solve
fini
save


!!!!!!!!!!!!!!!!!!!!!!!!!!!!!!!!!!!!!!!!!!!!!!!!!!!!!!!!!!!!!!!!!!!!!!!
!!!!!!!
/filname,%jobid%_struct
/prep7
et,1,45

/solu
antype,static,new
nsubst,1
time,1

/input,'Bdots\constraints',txt

fdel,all,all
ldread,forc,last,,,,%jobid%_em,rst
solve
fini
/post1
plnsol,s,eqv
save

/input,'Bdots\get_images',txt
```

The macro ‘mesh.txt’ meshes the specific geometry of the shutter using brick-type elements. B_mac.mac is a function to convert the magnetic field to a vector potential, which is then read into

ANSYS. This function is shown below. ‘constraints.txt’ places specific physical constraints on the shutter for static analysis. ‘get_images.txt’ saves images of different views and plots of interest, such as stress plots or eddy current distributions.

b_mac.mac

This function converts the magnetic field of interest to a corresponding vector potential and imposes it on the nodes. This function was originally written by A. Brooks for use in the general tile qualification macro.

```
!
! macro to set magnetic vector potential (in rectangular) to produce
uniform B field
! usage:  b_mac,bx,by,bz
!
*get,n,node,,num,min
*get,nnode,node,,count
*do,i,1,nnode
d,n,ax,(arg2*nz(n)-arg3*ny(n))/2.
d,n,ay,(arg3*nx(n)-arg1*nz(n))/2.
d,n,az,(arg1*ny(n)-arg2*nx(n))/2.
*get,n,node,n,nxth
*enddo
```

ANSYS Thermal Analysis Macro

The macro below is a single version of the thermal analysis macro. There are several versions, each with slight modifications to correspond with a particular situation. The macro below also calls several other macros, each of which will be described below. They will not be shown because they are unique to a given situation.

```
fini
/clear
jobid = 'type1'

/aux15
igesin,jobid,iges
/auto
/replot

/prep7

! Material Properties - 304 Stainless Steel
et,1,70
mp,dens,1,8000
mp,ex,1,193e9
mp,prxy,1,0.3
mp,kxx,1,18.
```

```
mp,alpx,1,18.e-6
mp,c,1,500.

/input,mesh,txt

!
! Thermal Loading
tem0=25
hflx=.13e6
tpulse=5
!
/view,1,1,1,1

allsel
fini
!!!!!!!!!!!!!!!!!!!!!!!!!!!!!!!!!!!!!!!!!!!!!!!!!!!!!!!!!!!!!!!!!!!!!!

/filnam,%jobid%_therm
!
/solu
antype,trans,new
nsubst,10
time,tpulse
!

/input,hflx_nodes,txt

sf,all,hflux,hflx
allsel
/replot
tunif,tem0
!
solve
fini
!
/post1
plnsol,temp
fini
save
!
!!!!!!!!!!!!!!!!!!!!!!!!!!!!!!!!!!!!!!!!!!!!!!!!!!!!!!!!!!!!!!!!!!!!!!
! change filname to avoid overwriting thermal solution
!
!
/filnam,%jobid%_struct
/prep7
et,1,45
fini
!
/solu
antype,static,new
```

```
nsubst,1
time,1
!

/input,constraints,txt

fdel,all,all
ldread,temp,last,,,,%jobid%_therm,rth
solve
fini
!
/post1
plnsol,s,eqv
save
/input,get_images,txt
```

The macro 'mesh.txt' meshes the specific geometry of the shutter using brick-type elements. 'hflx_nodes.txt' selects the nodes that are to have the heat flux applied to them. 'constraints.txt' places specific physical constraints on the shutter for static analysis. 'get_images.txt' saves images of different views and plots of interest, such as stress plots or eddy current distributions.

Python Ratcheting Script

Python was chosen for this script because it is a very simple language in which to program, it is easy to read, and it has some very powerful libraries. For this script PyLab was used for its simple graphing utilities.

```
from pylab import *

# Choose from list of most commonly used materials
print "Choose shutter material from list:"
print "  1. 304/316 Stainless Steel"
print "  2. 625 Inconel"
print "  3. User Specified"
print

mat = input("Material (number only): ")
if (mat == 1):
        emisSO = 0.44
        density = 8000.
        c = 500.
elif (mat == 2):
        emisSO = 0.24
        density = 8440.
        c = 481.4
else:
        emisSO = input("Emissivity of material: ")
        density = input("Density of material (kg/m^3): ")
        c = input("Specific heat of material (J/(kg*K)): ")
```

```
thickness = input("Enter thickness of shutter in mm: ")

temp = []
emisV = 0.8           # emissivity of vessel

numpulses = 15
pulselength = 5.      # seconds
pulseheat = 8.15e6    # Watts/m^2
T1 = 292.             # in Kelvins
dt = 1                # seconds

cdtime = 20.
thickness /= 1000. # Convert mm to m
Tmax = 0
Tpulse1 = 0
t = arange(0,numpulses*(pulselength + cdtime*60),dt)

# Calculate heating and find equillibrium temperature.
for i in range(0,numpulses):
        for j in range(0,int(pulselength/dt)):
            q = pulseheat * dt
            T1 += q /(c*thickness*density)
            temp.append(T1)
            if (T1 > Tmax): Tmax = T1

        if (Tpulse1 == 0): Tpulse1 = T1
        for j in range(0,int(cdtime*60./dt)):
            q = emisSO*emisV*5.67e-8*(T1**4-373**4)*dt/(emisSO+emisV-
emisSO*emisV)
            T1 -= q /(c*thickness*density)
            temp.append(T1)
            if (T1 > Tmax): Tmax = T1

# Output results.
print
print "Pulse length: " + str(pulselength) + " seconds"
print "Plasma heating: " + str(pulseheat) + " Watts/m^2"
print "Time between shots: " + str(cdtime) + " minutes"
print "Emissivity of the vessel: " + str(emisV)
print "Emissivity of the Shield: " + str(emisSO)
print "Temperature after 1 pulse: " + str(Tpulse1-273.15) + " C"
print "Equilibrium temperature: " + str(Tmax-273.15) + " C"

plot(t,temp)
suptitle('Temperature versus Time')
xlabel('time (s)')
ylabel('temperature (K)')
show()
```

Appendix

Table 4. List of shutter locations, background magnetic fields, and changes in magnetic fields.

Shutter	r [m]	Z [m]	B_x [T]	B_y [T]	B_z [T]	$B_x$dot [T/s]	$B_y$dot [T/s]	$B_z$dot [T/s]	Notes
Thomson	1.7	0	0.55	-0.44	-0.11	0	-130	-15	Constrained
Thomson	1.7	0	0.55	-0.44	-0.11	0	-130	-15	Unconstrained
Type 1	1.7	0	0.55	-0.40	-0.02	0	-125	10	None
Type 1	1.1	-1.53	0.85	0.18	-0.56	0	-165	-120	None
Type 2	1.55	-0.5	0.60	-0.58	-0.07	0	-170	-110	Closed
Type 2	1.55	-0.5	0.60	-0.07	-0.58	0	-110	-170	Open
Type 2	1.7	0	0.55	-0.40	-0.02	0	-125	10	Closed
Type 2	1.7	0	0.55	-0.02	-0.40	0	10	-125	Open
Type 3	1.1	-1.53	0.85	0.18	-0.56	0	-165	-120	None
Type 3	1.7	-0.35	0.55	-0.55	-0.16	0	-105	-25	None
Type 3	1.7	0	0.55	-0.40	-0.02	0	-125	10	None
Type 4	1.1	-1.53	0.85	0.18	-0.56	0	-165	-120	None
Type 5	1.7	0	0.55	-0.40	-0.02	0	-125	10	None
Type 6	1.1	-1.53	0.85	0.18	-0.56	0	-165	-120	Closed
Type 6	1.1	-1.53	0.85	-0.56	0.18	0	-120	-165	Open

Summary of Pointers

Detailed documentation files should be found with all scripts.

1. **Diagnostic Database** – This is the full database of diagnostics and sources regarding the diagnostics. The database may be updated at any time. It may be accessed through either of the pointers below.
    - P:\public\anonymous ftp public\boales\Diagnostics\NSTX Diagnostic Database.mdb
    - ftp://ftp.pppl.gov/pub/boales/Diagnostics/NSTX%20Diagnostic%20Database.mdb
2. **Images Generated by ANSYS Analyses** – The images that were generated and used in this report as well as any that were not included may be found at the sources below.
    - P:\public\anonymous ftp public\boales\Shutter Analysis\images
    - ftp://ftp.pppl.gov/pub/boales/Shutter%20Analysis/images/
3. **Python Ratcheting Script** – The Python Ratcheting Script and True Basic program that it was based on can be found at either of the sources below.
    - P:\public\anonymous ftp public\boales\Ratcheting
    - ftp://ftp.pppl.gov/pub/boales/Ratcheting/
4. **All ANSYS Scripts** – All of the scripts and .iges files used in the analyses can be found at either of the locations below.
    - P:\public\anonymous ftp public\boales\Shutter Analysis\Analyses
    - ftp://ftp.pppl.gov/pub/boales/Shutter%20Analysis/Analyses/

5. **Magnetic Field and Bdot Spreadsheet** – This spreadsheet interpolates the maximum Bdots and magnetic fields at any location inside NSTX and to a certain point beyond the boundary of the machine.
    - P:\public\anonymous ftp public\boales\Magnetic Fields\ Hatcher_Max_B_Calculation.xlsx
    - ftp://ftp.pppl.gov/pub/boales/Magnetic%20Fields/Hatcher_Max_B_Calculation.xlsx

If any of these pointers are broken, feel free to search the directory "P:\public\anonymous ftp public\boales\" or "ftp://ftp.pppl.gov/pub/boales/" for the file of interest. If you cannot find it, I apologize for the inconvenience.

6. **Reference calculation** – The detailed background magnetic field calculation can be found in Woolley's calculation completed CALC-131-03-00. The worst case disruption can be different for different shutter type – please see CALC-131-03-00 for details.

Since the shutters are treated as isolated components without any electrical connection to the global port plug or VV model, the assumption is thus eddy current in individual shutter is locally self-contained. There is little coupling during disruption between two adjacent shutters.